Coherent synthesis of genomic associations with phenotypes and home environments

Jesse R. Lasky[1,2], Brenna R. Forester[3], and Matthew Reimherr[4]

5    [1]Department of Biology
Pennsylvania State University
408 Life Sciences Building
University Park PA 16802-5301

10   [2]Correspondence: jrl35@psu.edu, Phone: (814) 863-5318, Fax: (814) 865-9131

[3]Nicholas School of the Environment
Duke University
450 Research Drive
15   Durham, NC 27708-0001

[4]Department of Statistics
Pennsylvania State University
411 Thomas Building
20   University Park PA 16802-5301

25   Running title: Synthesis of genome, environment, & phenotype

*Abstract*

30     Local adaptation is often studied via 1) multiple common garden experiments comparing performance of genotypes in different environments and 2) sequencing genotypes from multiple locations and characterizing geographic patterns in allele frequency. Both approaches aim to characterize the same pattern (local adaptation), yet the complementary information from each has not yet been coherently integrated into a

35     modeling framework. Here, we develop a genome-wide association model of genotype interactions with continuous environmental gradients (G×E), *i.e.* reaction norms. We employ an imputation approach to synthesize evidence from common garden and genome-environment associations, allowing us to identify loci exhibiting environmental clines where alleles are associated with higher fitness in home environments. Simulations

40     show our approach can increase power to detect loci causing local adaptation. In a case study on Arabidopsis thaliana, our approach reveals candidate genes for local adaptation based on known involvement in environmental stress response. Most identified SNPs exhibited home allele advantage and fitness tradeoffs along climate gradients, suggesting selective gradients maintain allelic clines. SNPs exhibiting G×E associations with fitness

45     were enriched in genic regions, putative partial selective sweeps, and G×E associations with an adaptive phenotype (flowering time). We discuss extensions for situations where only adaptive phenotypes other than fitness are available. Many types of data may point toward the loci underlying G×E and local adaptation; coherent models of diverse data provide a principled basis for synthesis.

## Introduction

50     Populations commonly exhibit phenotypic differences, often due to local adaptation to environment (Leimu & Fischer 2008; Hereford 2009). Local adaptation is defined as a genotype-by-environment interaction (G×E) for fitness that favors home genotypes (Kawecki & Ebert 2004). Local adaptation has long interested empirical and theoretical

55     biologists (Clausen *et al.* 1940, 1948; Levene 1953; Slatkin 1973). However, little is known about the genomic basis of local adaptation, such as genetic architecture, major molecular mechanisms, and the extent to which genomic divergence among populations is driven by local adaptation. Because local adaptation involves organismal responses to environmental gradients, understanding the mechanisms of local adaptation has important

60     applications in agriculture and biodiversity conservation under climate change (Aitken & Whitlock 2013; van Oppen *et al.* 2015; Lasky *et al.* 2015). Additionally, G×E are important in human phenotypes like disease (Anastasi 1958; Hunter 2005; Gage *et al.* 2016). Understanding the genomic basis of G×E is an emerging area of biomedical research (Thomas 2010; Keller 2014) as are the genomics of local adaptation (reviewed

65     by (Des Marais *et al.* 2013; Manel & Holderegger 2013; Tiffin & Ross-Ibarra 2014; Adrion *et al.* 2015; Bragg *et al.* 2015; Hoban *et al.* 2016)).

      A central question in local adaptation is whether selective gradients can maintain allelic clines at individual loci, or whether stochastic processes, like limited dispersal, are required to explain clines at individual loci causing local adaptation (Mitchell-Olds *et al.*

70     2007; Anderson *et al.* 2011b). If selective gradients cause rank changes in alleles with the highest relative fitness at an individual locus, selection may maintain a cline, a pattern known as genetic tradeoff or antagonistic pleiotropy (Ågren *et al.* 2013). Detecting loci

3

that exhibit antagonistic pleiotropy has been challenging, partly due to limited statistical power of approaches that conduct multiple tests of significance for opposing fitness

75     effects in different environments (Fournier-Level *et al.* 2011a; ANDERSON *et al.* 2013).

        Common garden experiments have long been employed to characterize genetic variation in phenotypes (Langlet 1971). In particular, reciprocal common gardens at multiple positions along environmental gradients are a powerful tool to reveal local adaptation (Clausen *et al.* 1940, 1948). One approach to identifying the loci underlying

80     local adaptation is to combine fitness data from multiple common garden experiments with genomic data (Lowry & Willis 2010; Fournier-Level *et al.* 2011a; Anderson *et al.* 2011a; Ågren *et al.* 2013). However, common gardens are logistically challenging and it is unclear how the typically small spatiotemporal scales of common gardens relate to the scales of processes that generate local adaptation in the wild (Weigel & Nordborg 2015).

85         An alternative to discovering genetic and ecological mechanisms of local adaptation is to study changes in allele frequency along environmental gradients (Hedrick *et al.* 1976; Tiffin & Ross-Ibarra 2014; Adrion *et al.* 2015; Bragg *et al.* 2015; Rellstab *et al.* 2015; Hoban *et al.* 2016). In this approach, known as a genome-environment association study, individuals are sequenced from multiple locations along environmental

90     gradients. Genetic markers and environmental gradients showing the strongest correlations are then considered as potentially involved in local adaptation (*e.g.* Hancock *et al.* 2008, 2011; ECKERT *et al.* 2010; Turner *et al.* 2010; Coop *et al.* 2010; Lasky *et al.* 2012; Jones *et al.* 2012; Fitzpatrick and Keller 2015). A challenge of both traditional association studies (genome-phenotype) and genome-environment association studies is

95     that the genomic variation is observational and is not experimentally randomized (as

opposed to linkage mapping with experimental crosses) (Devlin & Roeder 1999; Hancock *et al.* 2008; Kang *et al.* 2008; Nordborg & Weigel 2008). As a result, many loci may show spurious associations with phenotypes or with environment (Price *et al.* 2010; Schoville *et al.* 2012; Bragg *et al.* 2015). Spurious associations are particularly

100    problematic for environmental gradients that are spatially autocorrelated due to confounding with population structure (Schaffer & Johnson 1974). A technique for dealing with this confounding is to control for putative population structure when testing associations (Coop *et al.* 2010) by controlling for genome-wide (identity-in-state) similarity among accessions (Yoder *et al.* 2014; Lasky *et al.* 2014).

105        Understanding the genomic basis of adaptation may benefit from synthesizing lines of evidence, for example by combining multiple types of genome scans to strengthen the evidence that a locus is under selection (Lasky *et al.* 2014; Evans *et al.* 2014). For example, researchers have identified overlap between outliers for selection statistics and markers associated with putatively adaptive phenotypes (Horton *et al.* 2012)

110    or between SNPs associated with phenotypes and those associated with climate gradients (Berg & Coop 2014). (Lasky *et al.* 2015) used a Bayesian approach to combine associations with phenotype and environment, first calculating climate associations and then using each marker's association to determine the prior probability it was associated with G×E for adaptive phenotypes, yielding a posterior. Although combining multiple

115    lines of evidence is potentially useful, the quantitative approaches in past studies have often been *ad hoc* and lacked reasoned principles. Here we develop a modeling framework to conduct genome-wide association scans for G×E while coherently synthesizing multiple data types. Existing approaches to genome-wide association studies

(GWAS) with G×E (sometimes referred to as genome-wide interaction studies, GWIS)

120    have dealt with categorical nominal environments (Murcray *et al.* 2009; Thomas 2010; Korte *et al.* 2012; Gauderman *et al.* 2013; Marigorta & Gibson 2014), benefiting from the statistical convenience of modeling phenotypes in different environments as correlated traits (Falconer 1952). Association models have not been applied to G×E along continuous environmental gradients, such as modeling SNP associations with reaction

125    norms (Jarquín *et al.* 2014; Tiezzi *et al.* 2017). Despite the existence of studies where fitness was measured in multiple common gardens for diverse genotyped accessions (Fournier-Level *et al.* 2011a), studies where linkage mapping was conducted for fitness at multiple sites (Ågren *et al.* 2013), and studies where authors conducted association mapping for G×E effects on phenotypes (Li *et al.* 2014), we found no example of

130    association studies of G×E for fitness, which is the basis of local adaptation.

        The underlying processes generating local adaptation are the same regardless of whether genome-environment associations or common gardens are used for inference. Thus it is natural to synthesize these data. Furthermore, by combining datasets into a single inferential framework we may increase power and accuracy for detecting causal

135    loci. Here, we simultaneously leverage data from multiple common gardens and genome-environment associations. In the remainder, we describe our approach, present test cases using simulations and published data on *Arabidopsis thaliana* (hereafter Arabidopsis), and discuss extensions.

140    **Methods**

    *Genome-wide association study of G×E effects on fitness*

In common garden experiments, environment is often treated as a factor. When more than two gardens are conducted, variation among them may be considered in a more general fashion. For a given environmental gradient, each common garden may be located along

145     the gradient according to its conditions. Describing common gardens as such may be informative about the specific ecological mechanisms driving selective gradients, taking advantage of the ordered nature of gardens' environments. We leverage multiple common garden experiments to identify markers (single nucleotide polymorphisms, SNPs) that show the strongest G×E effects, loci where allelic state shows the strongest interaction

150     with environment in its association with fitness.

Local adaptation requires a genotype by environment interaction for fitness at the whole genome-level. Variation in individual phenotypes from multiple environments can be separated into components determined by genotype, environment, and G×E (Yates & Cochran 1938; Falconer 1952). To assess this interaction at an individual locus, one can

155     assume that the relative fitness of individual $i$ in a single location, $w_i$, satisfies the linear model

$$w_i = \alpha + \beta_E E_i + \beta_G G_{i,l} + \beta_{G \times E} G_{i,l} E_i + \varepsilon_i,$$

(eqn 1)

where $G_{i,l}$ is the genotype of individual $i$ at locus $l$ and $E_i$ is the value of a single

160     environmental variable at the location where $w_i$ was measured. The $\beta_E$ parameter gives the effect of environment on fitness and $\beta_G$ gives the effect of genotype on fitness. Our primary interest lies in the $\beta_{G \times E}$ parameter, which gives the strength and direction of G×E effects; $\beta_{G \times E}$ determines how responses to environmental gradients are mediated by

7

genotype. The term $\alpha$ gives the fitness intercept. We assume that the vector of errors, $\boldsymbol{\varepsilon}$,

165    can be expressed as

$$\boldsymbol{\varepsilon} = \boldsymbol{Ev} + \boldsymbol{e}$$

where $\boldsymbol{E}$ is a diagonal matrix of the environmental values, and

$$\boldsymbol{v} \sim N_n(0, \sigma^2_{G \times E}\, \boldsymbol{K}) \qquad \boldsymbol{e} \sim N_n(0, \sigma^2_e \boldsymbol{I}).$$

 (eqn 2)

170    Here $\boldsymbol{v}$ and $\boldsymbol{e}$ are independent. The matrix $\boldsymbol{K}$ is calculated as the genome-wide identity in

state for each pair of accessions (Kang *et al.* 2008). Random effects $\boldsymbol{v}$ are included

because a substantial portion of G×E may be associated with population structure (Lasky

*et al.* 2015); naively applying standard F-tests to assess the interaction effects can result

in a dramatic increase in false positive rates. To ameliorate this issue, the random effect $\boldsymbol{v}$

175    represents the genetic background interactions with environment (G×E, magnitude of

their variance determined by $\sigma^2_{G \times E}$), while $\boldsymbol{e}$ represents the independent and identically

distributed error in the model (variance determined by $\sigma^2_e$). However, it is important to

note that incorporating random effects may also decrease power when causal loci covary

with genomic background.

180

*Coherent synthesis of common gardens and genome-environment associations via*

*imputation*

We now tackle the goal of synthesizing genome-environment associations and G×E

observed in multiple common gardens, given that both patterns are expected to inform on

185    the same process of local adaptation. The challenge in synthesizing these approaches is

that genome-environment associations are purely observational and lack common garden

8

data. However, an implicit assumption in studies of genome-environment associations is that local adaptation occurs; if a common garden were conducted at each location where genotypes are collected, the home genotype would tend to be most fit. Here, we make this

190   assumption of genome-environment association studies explicit. A formal consequence of this assumption is an (imputed) observation of highest relative fitness for genotypes at home, which we combine with observed genomic marker and environment of origin data (Figure 1). Next, we scale relative fitness within each common garden so that the maximum observed fitness is given a relative fitness of unity, yielding a measure that can

195   be directly observed or imputed in each type of study (common garden and genome-environment association). For imputation, we then assume that each genotype collected from wild populations is locally adapted at its home and thus has a relative fitness = 1 (Figure 1). After imputation, we can calculate marker associations with G×E for fitness, where each fitness observation arises from either (A) observations on a given genotype

200   by common garden combination or (B) imputation on a given genotype collected from its natural home and subsequently sequenced.


*Comparing approaches and fitting models*

We compared four reaction norm approaches to genome-wide G×E association studies in

205   addition to a more common approach to genome associations with the home environment (genome-environment association). In Approach 1, we ignored potential confounding of population structure, using least squares to fit the model in eqn 1 where $\boldsymbol{\varepsilon}$ is normal, independent, and identically distributed (excluding random effects $\boldsymbol{v}$), but only including observed fitness data from common gardens and. excluding imputed fitness data. In

9

210  Approach 2, we again used a linear model but included imputed fitness data; these

imputations using information from the ancillary geographic data could possibly reduce

false positives. In Approach 3, we fit the full mixed-effects model (including random

effects *v*), but excluded imputed fitness. In Approach 4, we fit the full mixed-effects

model while including imputed fitness data. To test a genome-environment association

215  approach (Approach 5), we also compared associations between SNPs and home

environments used a mixed-effects model in an approach akin to traditional association

mapping but where environment is substituted for phenotype (Yoder *et al.* 2014; Lasky *et*

*al.* 2014).

To improve computation time for the mixed-model approaches (3 & 4), we used

220  the method of (Kang *et al.* 2010) and first fit the random effects with covariance

determined by kinship, and then fixed these effects while testing the effects of each SNP

on the phenotype. We included the environmental covariate effect in this initial step,

following the recommendation of (Kang *et al.* 2010) for fitting additional non-SNP

covariates. In other words, we first fit the model:

225  $$w_i = \alpha + \beta_E E_i + \varepsilon_i,$$

(eqn 3).

Eqn. 3 is the same as Eqn. 1 but with genetic effects omitted. We obtained parameter

estimates $\hat{\alpha}, \widehat{\beta_E}, \hat{\sigma}_e^2, \hat{\sigma}_{G \times E}^2$. We then take the variance parameter estimates and use them to

estimate the remaining slope coefficients in eqn 1 using generalized least squares.

230  Because inclusion of the $\beta_E$ term in ordinary least squares regression (Approaches 1-2)

led to poor model fit, we excluded the term from those approaches. We fit the discussed

mixed-model using Minimum Norm Quadratic Unbiased Estimation, MINQUE (Rao

10

1971; Brown 1976; Reimherr & Nicolae 2016). This approach is equivalent to restricted maximum likelihood, REML, but rephrased in a way that more fully exploits the linearity

235    of the model, resulting in a flexible framework that can be quickly computed.


*Simulation*

We used simulations to demonstrate how our imputation technique can improve power to identify loci causing G×E for fitness. To assess scenarios with varying strength of local

240    adaptation, we tested simulations of varying dispersal distances. (Forester *et al.* 2016) previously simulated local adaptation in a square two-dimensional 1024 x 1024 grid-cell landscape along a continuous environmental gradient, using the program CDPOP v1.2 (Landguth & Cushman 2010). (Forester *et al.* 2016) simulated 5,000 diploid individuals with 100 bi-allelic loci, one of which was under selection (99 neutral loci). All loci had a

245    0.0005 mutation rate per generation, free recombination, and no physical linkage. The authors ran 10 Monte Carlo replicates of the simulation for 1,250 generations, using the first 250 generations as a burn-in, with no selection imposed, to establish a spatial genetic pattern.

In the simulation, selection changed linearly along an environmental gradient,

250    with *AA* and *aa* genotypes favored at different ends of the gradient (North and South, Fig. S1). The selection strength of *s*=0.10 at extreme ends of the gradient was mediated through density-independent mortality determined by an individual's genotype at the selected locus, where *AA* experienced 0% mortality at the North extreme and *s* mortality at the South extreme, while *aa* genotypes experienced the opposite selection gradient. *Aa*

255    genotypes experienced uniform selection of *s*/2 across the gradient.


11

Mating pairs of hermaphroditic individuals and dispersal locations of offspring were chosen using a random draw from the inverse-square probability function of distance, truncated at a distance equal to $d$, the proportion of a landscape edge. We tested three values of $d$: 0.03, 0.1, and 0.25 (*i.e.* truncated at 31, 102, and 256 pixels,

260    respectively). These three values resulted in strong, moderate, and weak local adaptation, respectively, with the Pearson's correlation between selected locus and selective gradient equal to 0.28, 0.24, and 0.11, respectively. Individuals near landscape edges were unable to disperse or mate with individuals beyond the edge such that boundaries were not periodic.

265    The number of offspring produced from mating (fitness) was determined from a Poisson distribution ($\lambda = 4$), which produced an excess of individuals each generation, maintaining a constant population size of 5,000 individuals at every generation. Carrying capacity of the landscape surface was 5,000 individuals, and excess individuals were discarded once all 5,000 locations became occupied.

270    We sampled 250 individuals randomly from the 5,000 available. We then located four common gardens at equal intervals along the gradient, encompassing the extremes of the selection surface (Fig. S1). For the moderate dispersal and local adaptation scenario, we tested the effect of common gardens that sample only half the environmental gradient (Fig. S1). For the gardens, we subsampled 100 individuals from the full 250, and then

275    averaged fitness for 25 clones of each individual (each with the identical adaptive genotype of their parent clone) in each common garden using the above parameters for selection and fitness. After imputing fitness for the 250 individuals in their home environments, we had a total of 650 observations of fitness × location (250 imputed

12

observations from individuals sampled across the landscape + 400 real observations

280    arising from 100 clones in each of four common gardens). For both the simulations and

the *Arabidopsis* case study, we focus on the 1% of SNPs with the lowest p-values and

their role in local adaptation. In simulations with 100 SNPs, this was equivalent to the

lowest p-value SNP. To determine false positive rates in simulations, we calculated the

proportion of simulations for a given scenario where a neutral (as opposed to a causal)

285    SNP had the lowest p-value for $\beta_{G \times E}$.


*Model extensions*

Two extensions to our approach could increase its generality by treating unobserved

fitness as a parameter rather than using imputation. First, an alternative would be to treat

290    unobserved fitness of a genotype in its home environment as a free parameter. To

constrain estimates of unobserved fitness one could use informative priors, such that the

prior probability of relative fitness at home for each genotype would be monotonically

increasing, *i.e.* local adaptation is the most likely state, but minor maladaptation is

common. Inferences about unobserved fitness could be further constrained using

295    hierarchical models, such that home fitness parameters for multiple genotypes arise from

a common distribution (GELMAN & HILL 2007). Relaxing the assumption of perfect

local adaptation would also generate less biased, if less precise, parameter estimates for

$\beta_{G \times E}$, which are currently conservative because imputation of local adaptation for

maladapted genotypes will push $\beta_{G \times E}$ toward zero and weaken estimates for selective

300    gradients.

13

Second, when fitness is not measured, components of fitness (*e.g.* survival) or traits thought to be locally adaptive (*e.g.* physiological or behavioral) can be measured and used to infer the genomic basis of local adaptation. For example, instead of modeling SNP×environment associations with fitness, one could model SNP×environment

305    associations with components of fitness or adaptive traits measured in common gardens, and estimate unobserved traits for sequenced genotypes using informative priors. To be clear, in our case study of *Arabidopsis*, we had near but not complete lifetime fitness data (missing germination stage). Here we do not fit these model extensions to data, given the current computational challenge of fitting many more parameters in a Bayesian

310    framework.


*Case study: local adaptation to climate in* Arabidopsis thaliana

We applied these approaches to published data from studies of *Arabidopsis thaliana* in its native Eurasian range. Fournier-Level *et al.* (2011) conducted replicated common

315    gardens at four sites across Europe: Spain, England, Germany, and Finland (Figure 2). With these data, (Fournier-Level *et al.* 2011a; b; Wilczek *et al.* 2014) showed evidence that genotypes are locally adapted to their home temperature and moisture regimes and that alleles associated with high fitness in a given garden tended to be found nearer to that garden than alternate alleles, suggesting these loci were involved in local adaptation. At

320    each site the authors transplanted 157 accessions (59 in the case of Finland) on a date in the fall matched to germination of local winter-annual natural populations (Fournier-Level *et al.* 2011a). The authors calculated survival (out of individuals surviving transplant) and average fecundity (where individuals that died before reproducing had

14

fecundity zero) giving an estimate of absolute fitness (excluding the seed to seedling

325      transition) (Fournier-Level *et al.* 2011a).

These accessions were part of a panel of 1,307 accessions from around the globe that were genotyped at ~250k SNPs using a custom Affymetrix SNP tiling array (AtSNPtile1), with 214,051 SNPs remaining after quality control (Figure 2) (Horton *et al.* 2012). This array was generated by resequencing 19 diverse ecotypes from across the

330      range of Arabidopsis (Kim *et al.* 2007). Of the 1,307 genotyped accessions, we used 1,001 accessions that were georeferenced and likely not contaminant lines (Anastasio *et al.* 2011), in addition to being from the native range in Eurasia (Hoffmann 2002; Lasky *et al.* 2012b), and excluding potentially inaccurate high altitude outliers (i.e. > 2000 m). After imputing fitness for accessions in their home environments we had a total of 1,531

335      observations of fitness × location (1001 imputed observations + 530 real observations). We removed from association tests SNPs having minor allele frequency (MAF) below 0.01, though we also considered a more conservative threshold of MAF = 0.1.

We used climate data compiled previously (Lasky *et al.* 2012b) from published global climate datasets (Hijmans *et al.* 2005; Zomer *et al.* 2008). Here we focus on four

340      climate variables that differ among common gardens, are not strongly correlated, and may be involved in local adaptation: minimum temperature of the coldest month, average monthly minimum temperature in the growing season, coefficient of variation of monthly growing season precipitation, and aridity index.

345      *Genome-wide G×E associations*

15

We separately tested for each SNP's interaction with each of the four environmental variables. For each of the four approaches using common garden data we fit a model for each combination of SNP and environmental variable. To characterize the types of patterns identified by our approach, we studied variation in the SNPs in the 0.01 lower

350 tail of p-values for the hypothesis test that $\beta_{G \times E} = 0$ (the coefficient for SNP×environment effects on fitness) for each climate gradient. We considered whether these SNPs showed patterns consistent with home genotype advantage via changes in the allele with greatest relative fitness along the environmental gradient (*i.e.* local adaptation via antagonistic pleiotropy) versus a pattern where $\beta_{G \times E}$ merely involved changes in fitness difference

355 between alleles (such as conditional neutrality or variance changing G×E), the latter of which cannot stably maintain local adaptation. For these SNPs, we calculated whether the direction of allelic differentiation along environmental gradients was consistent with the sign of $\beta_{G \times E}$. For example, if one allele was more common in accessions from warmer locations, we assessed whether that same allele showed an increase in relative fitness in

360 warmer common gardens.

Next, we assessed whether our model predicted that different alleles were most fit in the two common gardens at either extreme of a climate gradient, *i.e.* whether the SNP was associated with rank changes in fitness that are consistent with antagonistic pleiotropy. For example, if one allele was estimated to be most fit in the coldest common

365 garden, we determined whether a different allele was estimated to be most fit in the warmest common garden. Furthermore, we also quantified similarity (rank correlation in SNP scores and proportion of SNPs common to the strongest 0.01 tail of associations) between results from our G×E approach versus those from other recent studies of

16

association with home climate in Arabidopsis (Hancock *et al.* 2011; Lasky *et al.* 2012b,

370     2014).

*Enrichment of strong SNP×environment associations across the genome*

We studied whether loci we identified as likely being involved in local adaptation

exhibited supportive patterns in ancillary datasets. First, to assess whether our association

375     approach is capable of identifying the signal of local adaptation rather than spurious

background associations, we tested for enrichment of SNPs in genic versus intergenic

regions. These tests are based on the hypothesis that loci involved in adaptation are on

average more likely to be found near genes and linked to genic variation, in comparison

with loci evolving neutrally (Hancock *et al.* 2011; Lasky *et al.* 2012b). For a test statistic,

380     we calculated the portion of SNPs in the 0.01 lower p-value tail that were genic versus

intergenic.

Second, we hypothesized that locally-adaptive alleles may have been subject to

partial (local) selective sweeps, especially given that much of Arabidopsis' Eurasian

range was recently colonized following the last glacial maximum. We tested for an

385     enrichment of significant (alpha = 0.05) pairwise haplotype sharing (PHS, (Toomajian *et*

*al.* 2006)) in the SNPs (using PHS calculated by Horton et al. 2012) showing the greatest

evidence of G×E for fitness. We also tested evidence that these SNPs are enriched for

significant (alpha = 0.05) integrated extended haplotype homozygosity (standardized,

iHS (Voight *et al.* 2006)), an additional metric of partial sweeps. We used ancestral SNP

390     allele determinations from (Horton *et al.* 2012) (based on alignment with the *Arabidopsis*

*lyrata* genome) and the R package 'rehh' to calculate iHS (Gautier *et al.* 2012).

17

Third, we also studied whether loci we identified were associated with plasticity in flowering time, a trait that plays a major role in local adaptation to climate in plants (Hall & Willis 2006; Franks *et al.* 2007; Keller *et al.* 2012; Lowry *et al.* 2014). Recently

395    (Li *et al.* 2014) tested the flowering time response of 417 natural accessions to simulated warming (up to ~4ºC), and then identified SNP associations with changes in flowering time across treatments, G×E for flowering time. We tested whether SNPs we identified as having SNP×environment interactions for fitness (0.01 lower p-value tail) were enriched in nominally significant associations (alpha = 0.05) with G×E for flowering time.

400    To generate a null expectation for each enrichment while maintaining a signal of linkage disequilibrium in the null model, we circularly permuted SNP categories (*e.g.* as genic versus intergenic, having significant iHS or not) along the genome and recalculated the test statistics 10,000 times (Hancock *et al.* 2011; Lasky *et al.* 2012b).

405    **Results**

We compared four approaches to genome-wide G×E association study and one approach for genotype-environment association. Approach 1 used only observed (excluding imputed) fitness data, but no correction for population structure. Approach 2 used observed and imputed fitness data, and no correction for population structure. Approach 3

410    fitted the full mixed-effects model, but only including observed fitness data from common gardens, excluding imputed fitness. Approach 4 fitted the full mixed-effects model while including both observed and imputed fitness data. Approach 5 used a mixed model of genotype associations with environment (no common garden data).

415     *Simulations*

Across dispersal scenarios, we found that mixed models decreased false positive rates
and increased accuracy of inference as to the SNPs driving G×E for fitness (Figure 3).
When dispersal was highest and local adaptation weakest, all approaches exhibited an
increase in false positives compared to the moderate dispersal scenario. Among the

420     approaches using common garden data (Approaches 1-4), the mixed models generally
had low false positive rates and thus high true positive rates. Based on the low false
positive rates and low p-values for causal SNPs in Approach 3, common garden data
were a clear source of statistical power to identify causal SNPs (Figure 3). Including
imputed data (Approach 4) further reduced false positive rates and resulted in no false

425     positives under the two lower dispersal scenarios. Genotype-environment associations
that did not use common garden data (Approach 5) had similarly low false positive rates.
However, common garden data combined with imputations (Approach 4) yielded
stronger inference for SNPs driving G×E; causal SNPs had lower p-values (Figure 3,
median causal SNP p for low, med., high dispersal scenarios: $3.2 \times 10^{-6}$, $4.5 \times 10^{-13}$,

430     $7.4 \times 10^{-7}$) compared to ignoring common garden data (Approach 5, median causal SNP p
for low, med., high dispersal scenarios: $2.3 \times 10^{-7}$, $1.9 \times 10^{-10}$, $1.2 \times 10^{-5}$). Under a scenario
of medium dispersal and common gardens that only covered half the gradient, false
positive rates were elevated for approaches excluding fixed effects (Approaches 1-2) or
excluding imputations (Approach 3) but not when imputations and random effects were

435     included (Approach 4, Figure S4).

*Case study on Arabidopsis*

19

We found that simple linear model tests (Approaches 1-2) of SNP×environment interactions were highly enriched in very low p-values (Figure S5) relative to the

440    theoretical expectation. After incorporating the kinship×environment random effects (but excluding imputed fitness observations, Approach 3), we found that SNP×environment associations with fitness were closer to the theoretical expectation but still highly enriched in low p-values for three climate variables. After incorporating imputed fitness observations into the mixed model (Approach 4, right column, Figure S5), we found p-

445    value distributions hewed closer to the theoretical expectation and were slightly conservative (under-enriched in low p-values) for two climate variables. These approaches tended to identify different SNPs as having the strongest SNP×environment associations with fitness (Table S5).

        Based on the results of our simulations and the p-value distributions noted above,

450    we focus the remainder of analyses on results from mixed models with imputed fitness included (Approach 4). We found that climate variables differed in the importance of kinship-climate interaction associations with fitness (proportion of variance in fitness explained by random effects $v$), suggesting that population structure in Arabidopsis is more strongly correlated with some climatic axes of local adaptation (G×E for fitness)

455    compared to other climate gradients. For growing season minimum temperatures, kinship×environment interactions explained most of the variation in fitness ($R^2 =0.78$, Table 1, row 3). By contrast, kinship×environment interactions for fitness were weaker along a gradient in winter minimum temperature ($R^2 =0.07$).

        Approach 4 tended to identify SNPs where SNP×environment interactions

460    favored alleles in climates where they were relatively more common, that is, the sign of

20

allelic differences in home climates were mirrored by the sign of fitted mixed model SNP×environment associations with relative fitness (Table 1, row 1, and see outlier examples in Figure 4). In addition to characterizing SNP×environment associations, we tended to identify SNPs where we estimated a rank change in relative fitness for alternate

465 alleles along the environmental gradient between the two extreme common gardens (where the fitted model expectation was that the allele with higher fitness at one extreme common garden differed from the allele with higher fitness at the other extreme, Table 1, row 2). It appeared that the proportion of SNPs expected to show rank changes in relative fitness among the common gardens was related to how much of each climate variable's

470 range was covered by gardens (Table 1, row 4). Thus the common gardens may have been limited in their ability to capture rank changing of alleles at some loci involved in local adaptation to aridity and growing season cold.

We found non-random, but very weak overlap between the SNPs we identified and those outliers in previous analyses (Hancock *et al.* 2011; Lasky *et al.* 2012b, 2014).

475 When considering mixed model (Lasky *et al.* 2014) or partial Mantel (Hancock *et al.* 2011) SNP associations with the same climate variables (genome-environment associations with no common garden data), we found significant overlap among the previously identified SNPs in the 0.01 lower tail of p-values versus those in the 0.01 tail identified here (permutation test, all $p<0.05$, Table S6). However, rank correlations

480 among SNP scores from previous approaches versus our current approach were very weak (all rho < 0.2, Table S6).

21

*SNP×environment associations with fitness are enriched in regions suggestive of local adaptation*

485   To assess whether our approach identified certain types of SNPs, we tested for

enrichment of genic and intergenic regions for SNP×environment effects on fitness

(again focusing on Approach 4: mixed model including imputations). We found that

SNP×environment interactions for fitness were significantly enriched in genic regions

(Table 2; for reference, SNPs identified via Approach 2, including imputation but without

490   random effects, were not significantly enriched in genic regions). Additionally, we found

that SNP×environment interactions for fitness were enriched for high pairwise haplotype

sharing (PHS) and high integrated extended haplotype homozygosity (iHS, Table 2).

Finally, SNPs associated with G×E for flowering time response to growing temperature

(Li *et al.* 2014) tended to also have strong SNP×growing season minimum temperature

495   interactions for fitness (p < 0.0002) but not for other climate variables. (Table 2)

Enrichments reported above did not change qualitatively (with respect to statistical

significance) when we only considered SNPs with MAF > 0.1.


*SNP×environment associations with fitness identify genes potentially involved in local*

500   *adaptation*

Our approach identified a number of strong candidates for local adaptation at the top of

lists of SNPs with the strongest SNP×environment associations with relative fitness

(Tables S1-S4). For example, the top SNP associated with aridity interaction effects on

fitness (chr. 4, position 11005059) fell within LESION SIMULATING DISEASE 1

505   (LSD1), which affects a number of traits in Arabidopsis, including survival and fecundity

under drought (Wituszyńska *et al.* 2013; Szechyńska-Hebda *et al.* 2016) (Figure 4), while the third SNP (chr. 2, position 7592008) fell within ATMLO8, MILDEW RESISTANCE LOCUS O 8, homologous with barley MLO which controls resistance to the fungal pathogen powdery mildew (Büschges *et al.* 1997). The top SNP associated with winter

510    cold interaction effects on fitness (chr. 5, position 7496047) falls within coding region of WRKY38, involved in the salicylic acid pathway and pathogen defense (Kim *et al.* 2008), and was the same locus identified as most strongly associated with multivariate climate in Lasky et al. (2012) (Figure 4). The top SNP associated with variability in growing season precipitation interaction effects on fitness (chr. 2, position 18504858)

515    falls 380 bp from ABA HYPERSENSITIVE GERMINATION 11, AHG11, which mediates the effect of abscisic acid (ABA), a major hormone of abiotic stress response, on germination (Murayama *et al.* 2012). The fifth highest SNP (and second highest locus) associated with growing season cold interaction effects on fitness (chr. 3, position 8454439) fell within ABERRANT LATERAL ROOT FORMATION 5, ALF5, a gene

520    that confers resistance to toxins (Diener *et al.* 2001) belonging to the MATE gene family, which play a variety of roles responding to environment (Shoji 2014).

**Discussion**

Genetic variation in environmental responses (G×E) is ubiquitous but its genetic and

525    physiological basis and role in local adaptation is poorly understood. Replicated common garden experiments and genome scans for loci exhibiting evidence for local adaptation have been important in understanding the genetic basis of G×E and local adaptation (Hancock *et al.* 2008; ECKERT *et al.* 2010; Turner *et al.* 2010; Fournier-Level *et al.* 2011a; Lasky *et al.* 2012b; Ågren *et al.* 2013; Evans *et al.* 2014; Lasky *et al.* 2015).

530  However, the complementary information in common gardens and geographic variation in allele frequency have not been coherently synthesized. Previous association studies of G×E have modeled discrete, categorical environmental effects (Murcray *et al.* 2009; Thomas 2010; Korte *et al.* 2012; Marigorta & Gibson 2014). The modeling of G×E across discrete, categorical environments is typically conducted, in part, for mathematical

535  convenience, as such a treatment allows the use of models designed for multiple phenotypes, where the same phenotype in different environments is considered as multiple phenotypes (Falconer 1952).

We demonstrated an approach to association study of G×E for fitness and an imputation technique that allowed us to coherently synthesize evidence from common

540  gardens and genome-environment associations. Our imputation method relied on making explicit the implicit assumption of local adaptation that underlies genome-environment association studies (Coop *et al.* 2010; Hancock *et al.* 2011; Lasky *et al.* 2012b). Using simulation, we demonstrated that this imputation can increase power to identify SNPs causing G×E for fitness and local adaptation. Our approach also identified strong

545  candidate genes in Arabidopsis associated with SNPs that exhibit fitness tradeoffs along climate gradients such that locally common alleles had greater relative fitness.

The relative information on selective and adaptive genetic mechanisms contained in the two datasets (common garden, geographical genomic) for a given system will be determined by several factors. First, the power of common gardens depends on the range

550  of sampled covariates (genotype and environment). We found evidence with both our simulations and empirical case study that greater coverage of environmental gradients can increase power to detect loci under selection by selective gradients. Similarly, power

24

may be enhanced by including in common gardens a range of variation at locally adaptive loci using diverse germplasm from across gradients. However, confounding between

555     population structure and adaptive loci and alternate mechanisms of local adaptation across regions suggest that regional stratification in scans for local adaptation may be more powerful (e.g. (Horton *et al.* 2016)). Additionally, the power of common gardens is influenced by the match between conditions in gardens and long-term natural selective gradients that give rise to local adaptation (Weigel & Nordborg 2015), and the heritability

560     of adaptive traits and fitness. The information contained in genome-environment associations (and hence imputed fitness data here), is influenced by the strength of local adaptation in sampled populations (Figure 3), which itself is determined by steepness of selective gradients, the level of gene flow, and time populations have had to evolve toward equilibrium allele frequencies (Yeaman & Whitlock 2011; Lotterhos & Whitlock

565     2014; Forester *et al.* 2016). It is important to recognize that our simulations covered a limited range of the parameter space relevant in nature (genetic architecture of local adaptation, dimensionality of environmental selective gradients, etc.). Here, populations were given time to reach equilibrium (Forester et al. 2016), which likely enhanced the power of genotype-environment associations compared to scenarios common in nature

570     where populations may still be responding to long-term environmental changes such as glacial cycles. Apart from information on genetic mechanisms of G×E for fitness, common gardens afford a more direct opportunity to study phenotypes under selection, as opposed to genotype–environment associations where information on phenotype is limited to gene annotations.

575     Above we described a method of imputation based on the assumption of local

adaptation, *i.e.* home genotypes had greater fitness than away genotypes. However, local

adaptation in nature is typically imperfect, such that the optimal genotype for a given

location might not be the home genotype (Leimu & Fischer 2008; Hereford 2009). Local

adaptation may not occur due to immigration of maladaptive alleles (Slatkin 1973),

580     limited genetic variation (Barton 2001), temporal environmental shifts, and other

processes (Bridle & Vines 2007). Thus our imputation can be considered a heuristic to be

improved by further development.


*Genotype-by-environment interactions in genome-wide association studies*

585     Recent advances in association models have included explicit modeling of G×E (Murcray

*et al.* 2009; Thomas 2010; Korte *et al.* 2012; Marigorta & Gibson 2014; Li *et al.* 2014;

Kooperberg *et al.* 2016; Windle 2016), but to our knowledge there are no published

genome-wide association studies accounting for SNP interactions with continuous

environmental gradients (a reaction norm approach, cf. Jarquín *et al.* 2014; Tiezzi *et al.*

590     2017). By employing a reaction norm approach to G×E (as we did here), models can be

applied to prediction at new sites, which is not possible using correlated trait approaches

to G×E (Falconer 1952; Korte *et al.* 2012) where sites are treated as idiosyncratic. Some

of the aforementioned categorical treatments of SNP×environment interactions were used

in association studies for human disease. However, many of the environmental variables

595     that may mediate genetic risk of disease are continuous in nature, such as exposure to

ultraviolet radiation and tobacco smoke. Future research on local adaptation and human

disease may benefit from exchange of approaches given the shared importance across

disciplines of understanding the genomic basis of G×E.

600    *Case study on* Arabidopsis thaliana

Our approach identified many SNPs where allelic variation was associated with rank-

changing relative fitness tradeoffs along climate gradients (*e.g.* all 214 of the SNPs with

strongest interaction, *i.e.* 0.001 quantile, with winter minimum temperature association

for fitness), loci where selective gradients may stably maintain population differentiation

605    (Anderson *et al.* 2011b; Ågren *et al.* 2013). Studies of local adaptation genomics often

find limited evidence for loci with antagonistic pleiotropy. A previous study of the

common garden data used here (Fournier-Level *et al.* 2011a) found that the SNPs with

the strongest association with fitness in one common garden were rarely among those

with the strongest associations in another garden, which the authors interpreted as

610    evidence for conditional neutrality. However, the fact that a locus is not among the

strongest associated with fitness at an individual site does not indicate the locus is neutral

at that site, it may simply be under relatively weaker selection (see Figure S6 for example

illustration). By contrast with previous approaches that model phenotypes at a single site,

our model was explicitly focused on detecting alleles with the strongest evidence for

615    SNP×climate interactions favoring home alleles. Thus our explicit model of G×E is more

likely to detect loci with patterns indicative of antagonistic pleiotropy compared with

approaches that model fitness in a single common garden at a time, approaches that do

not model G×E.

27

Local adaptation may often involve complex traits governed by many loci. Loci

620     exhibiting antagonistic pleiotropy and loci exhibiting G×E but no tradeoffs (variance

changing or conditional neutrality) may both underlie genome-level local adaptation.

Note that our study, like that of (Fournier-Level *et al.* 2011a) is based on association

mapping, which may suffer from identification of more false positives compared with

linkage mapping approaches (HALL *et al.* 2010; ANDERSON *et al.* 2013; Ågren *et al.*

625     2013). Follow-up experimental study of phenotypic effects of variation at individual loci

is required to confirm the results of association mapping (Verslues *et al.* 2014;

Broekgaarden *et al.* 2015).

We found evidence that SNP×climate interaction effects on fitness were enriched

in genic regions, suggesting that our model captured a signal of local adaptation rather

630     than population structure. We found that enrichments in genic SNPs only emerged after

using a mixed model to control for the putative effects of population structure (genome-

wide similarity), suggesting that the genic-enriched patterns of divergence we modeled

were not simply associated with overall patterns of among-population divergence. This

enrichment is consistent with other findings in Arabidopsis (Hancock *et al.* 2011; Lasky

635     *et al.* 2012b) and other species ((Coop *et al.* 2009; Fumagalli *et al.* 2011; Lasky *et al.*

2015), but see (Pyhäjärvi *et al.* 2013)). We do not interpret this enrichment as indicating

that changes in amino acid sequences are more important than regulatory evolution in

local adaptation, but rather as supporting the hypothesis that local adaptation is more

likely to involve sequence evolution near genes as opposed to at locations farther from

640     genes, where many intergenic SNPs are found.

We found evidence that loci we identified as candidates were enriched in evidence for partial selective sweeps (PHS and iHS statistics), suggesting that recent sweeps in particular environments are an important mode of local adaptation (Voight *et al.* 2006; Toomajian *et al.* 2006). These local sweeps may be expected based on the range

645  dynamics of Arabidopsis, which has colonized much of its Eurasian range following the retreat of glaciers (Sharbel *et al.* 2000), a process that likely involved recent local adaptation. It is important to note that extended haplotype patterns suggestive of partial sweeps may occur at the shoulders (away from causal loci) of complete sweeps (Schrider *et al.* 2015), thus caution is warranted in attributing our observed PHS and iHS

650  enrichment to localized sweeps versus global sweeps at nearby loci.

We found significant overlap between SNPs associated with G×E for fitness along growing season cold gradients and SNPs associated with G×E for flowering time across growing season temperature treatments (Li *et al.* 2014). Our findings suggest that evolution of plasticity in flowering time is a mechanism of local

655  adaptation along growing season temperature gradients and that our model has captured the signal of this adaptation. For organisms inhabiting seasonal environments, timing of the life cycle can have large impacts on fitness. Previous common garden experiments have provided strong evidence that flowering time is a central trait involved in local adaptation (Hall & Willis 2006; Franks *et al.* 2007;

660  Keller *et al.* 2012; Lowry *et al.* 2014) with molecular study further supporting the role of flowering time (Stinchcombe *et al.* 2004; Caicedo *et al.* 2004; Shindo *et al.* 2005; Lovell *et al.* 2013) and the role of plasticity (Fraser 2013; Lasky *et al.* 2014) in local adaptation.

665     Though there was overlap with signal identified by previous approaches using the same data (Hancock *et al.* 2011; Lasky *et al.* 2012b, 2014), overlap was generally weak, indicating our approach identified distinct loci as causing local adaptation. In our case study on Arabidopsis, the SNPs that exhibited the strongest evidence for SNP×climate interaction effects on fitness often fell within the coding regions of strong candidate genes based on known roles in environmental responses, suggesting our

670     approach is a useful for identifying loci underlying local adaptation.


*Conclusions*

Local adaptation to environment involves genotype-by-environment interactions for

675     fitness. Genome-wide association studies are a promising approach for identifying the genomic basis of local adaptation and G×E. Additional approaches like genome-wide expression profiling may also be useful for uncovering the genomic basis of local adaptation (Des Marais *et al.* 2013). Future approaches that use a principled basis for quantitative synthesis of patterns in multiple data types (Levy Karin *et al.* 2017) may

680     enhance our ability to characterize adaptation in an integrative fashion.


**Acknowledgements**

We thank David Lowry, Thomas Juenger, and several anonymous reviewers for comments on earlier versions of this manuscript.

685

**References**

Adrion JR, Hahn MW, Cooper BS (2015) Revisiting classic clines in Drosophila melanogaster in the age of genomics. *Trends in Genetics*.

690     Ågren J, Oakley CG, McKay JK, Lovell JT, Schemske DW (2013) Genetic mapping of adaptation reveals fitness tradeoffs in Arabidopsis thaliana. *Proceedings of the National Academy of Sciences*, **110**, 21077–21082.

Aitken SN, Whitlock MC (2013) Assisted Gene Flow to Facilitate Local Adaptation to Climate Change. *Annual Review of Ecology, Evolution, and Systematics*, **44**,

695       367–388.

Anastasi A (1958) Heredity, environment, and the question" How?". *Psychological Review*, **65**, 197.

Anastasio AE, Platt A, Horton M *et al.* (2011) Source verification of mis-identified Arabidopsis thaliana accessions. *The Plant Journal*, **67**, 554–566.

700     Anderson JT, Lee C-R, Mitchell-Olds T (2011a) Life history QTLs and natural selection on flowering time in Boechera stricta, a perennial relative of Arabidopsis. *Evolution; international journal of organic evolution*, **65**, 771–787.

ANDERSON JT, LEE C-R, RUSHWORTH CA, COLAUTTI RI, MITCHELL-OLDS T (2013)

705       Genetic trade-offs and conditional neutrality contribute to local adaptation. *Molecular Ecology*, **22**, 699–708.

Anderson JT, Willis JH, Mitchell-Olds T (2011b) Evolutionary genetics of plant adaptation. *Trends in Genetics*, **27**, 258–266.

Barton NH (2001) Adaptation at the edge of a species' range. *SPECIAL*

710       *PUBLICATION-BRITISH ECOLOGICAL SOCIETY*, **14**, 365–392.

Berg JJ, Coop G (2014) A Population Genetic Signal of Polygenic Adaptation. *PLoS Genet*, **10**, e1004412.

Bragg JG, Supple MA, Andrew RL, Borevitz JO (2015) Genomic variation across landscapes: insights and applications. *New Phytologist*, n/a-n/a.

715　Bridle JR, Vines TH (2007) Limits to evolution at range margins: when and why does adaptation fail? *Trends in Ecology & Evolution*, **22**, 140–147.

Broekgaarden C, Bucher J, Bac-Molenaar J *et al.* (2015) Novel Genes Affecting the Interaction between the Cabbage Whitefly and Arabidopsis Uncovered by Genome-Wide Association Mapping. *PLoS ONE*, **10**, e0145124.

720　Brown KG (1976) Asymptotic Behavior of Minque-Type Estimators of Variance Components. *Ann. Statist.*, 746–754.

Büschges R, Hollricher K, Panstruga R *et al.* (1997) The Barley Mlo Gene: A Novel Control Element of Plant Pathogen Resistance. *Cell*, **88**, 695–705.

Caicedo AL, Stinchcombe JR, Olsen KM, Schmitt J, Purugganan MD (2004) Epistatic
725　interaction between Arabidopsis FRI and FLC flowering time genes generates a latitudinal cline in a life history trait. *PROCEEDINGS OF THE NATIONAL ACADEMY OF SCIENCES OF THE UNITED STATES OF AMERICA*, **101**, 15670–15675.

Clausen J, Keck DD, Hiesey WM (1940) Experimental Studies on the Nature of
730　Species. I. Effect of Varied Environments on Western North American Plants. Carnegie Institution of Washington Publication No. 520. *Washington, DC*.

Clausen J, Keck DD, HIESEY WM (1948) Experimental studies on the nature of species. III. Environresponses of climatic races of Achillea. *Experimental*

*studies on the nature of species. III. Environresponses of climatic races of*

735 *Achillea.*

Coop G, Pickrell JK, Novembre J *et al.* (2009) The Role of Geography in Human

Adaptation. *PLoS Genet*, **5**, e1000500.

Coop G, Witonsky D, Di Rienzo A, Pritchard JK (2010) Using Environmental

Correlations to Identify Loci Underlying Local Adaptation. *Genetics*, **185**,

740 1411–1423.

Des Marais DL, Hernandez KM, Juenger TE (2013) Genotype-by-Environment

Interaction and Plasticity: Exploring Genomic Responses of Plants to the

Abiotic Environment. *Annual Review of Ecology, Evolution, and Systematics*,

**44**, 5–29.

745 Devlin B, Roeder K (1999) Genomic Control for Association Studies. *Biometrics*, **55**,

997–1004.

Diener AC, Gaxiola RA, Fink GR (2001) Arabidopsis ALF5, a Multidrug Efflux

Transporter Gene Family Member, Confers Resistance to Toxins. *The Plant*

*Cell*, **13**, 1625–1637.

750 ECKERT AJ, BOWER AD, GONZÁLEZ-MARTÍNEZ SC *et al.* (2010) Back to nature:

ecological genomics of loblolly pine (Pinus taeda, Pinaceae). *Molecular*

*Ecology*, **19**, 3789–3805.

Evans LM, Slavov GT, Rodgers-Melnick E *et al.* (2014) Population genomics of

Populus trichocarpa identifies signatures of selection and adaptive trait

755 associations. *Nat Genet*, **46**, 1089–1096.

Falconer DS (1952) The Problem of Environment and Selection. *The American Naturalist*, **86**, 293–298.

Fitzpatrick MC, Keller SR (2015) Ecological genomics meets community-level modelling of biodiversity: mapping the genomic landscape of current and future environmental adaptation. *Ecology Letters*, **18**, 1–16.

Forester BR, Jones MR, Joost S, Landguth EL, Lasky JR (2015) Data from: Detecting spatial genetic signatures of local adaptation in heterogeneous landscapes.

Forester BR, Jones MR, Joost S, Landguth EL, Lasky JR (2016) Detecting spatial genetic signatures of local adaptation in heterogeneous landscapes. *Molecular Ecology*, **25**, 104–120.

Fournier-Level A, Korte A, Cooper MD *et al.* (2011a) A Map of Local Adaptation in Arabidopsis thaliana. *Science*, **334**, 86–89.

Fournier-Level A, Korte A, Cooper MD *et al.* (2011b) Data from: A map of local adaptation in Arabidopsis thaliana.

Franks SJ, Sim S, Weis AE (2007) Rapid evolution of flowering time by an annual plant in response to a climate fluctuation. *Proceedings of the National Academy of Sciences*, **104**, 1278–1282.

Fraser HB (2013) Gene expression drives local adaptation in humans. *Genome Research*, **23**, 1089–1096.

Fumagalli M, Sironi M, Pozzoli U *et al.* (2011) Signatures of Environmental Genetic Adaptation Pinpoint Pathogens as the Main Selective Pressure through Human Evolution. *PLoS Genet*, **7**, e1002355.

760

765

770

775

34

Gage SH, Davey Smith G, Ware JJ, Flint J, Munaf� MR (2016) G = E: What GWAS Can Tell Us about the Environment. *PLoS Genet*, **12**, e1005765.

780    Gauderman WJ, Zhang P, Morrison JL, Lewinger JP (2013) Finding Novel Genes by Testing G×E Interactions in a Genomewide Association Study. *Genetic epidemiology*, **37**, 603–613.

Gautier, M., Vitalis, R. (2012) rehh: An R package to detect footprints of selection in genome-wide SNP data from haplotype structure. *Bioinformatics*, **0**, accepted.

785    GELMAN A, HILL J (2007) *Data Analysis Using Regression and Multilevel/Hierarchical Models*. Cambridge University Press, Cambridge.

HALL MC, LOWRY DB, WILLIS JH (2010) Is local adaptation in Mimulus guttatus caused by trade-offs at individual loci? *Molecular Ecology*, **19**, 2739–2753.

Hall MC, Willis JH (2006) DIVERGENT SELECTION ON FLOWERING TIME

790        CONTRIBUTES TO LOCAL ADAPTATION IN MIMULUS GUTTATUS POPULATIONS. *Evolution*, **60**, 2466–2477.

Hancock AM, Brachi B, Faure N *et al.* (2011) Adaptation to Climate Across the Arabidopsis thaliana Genome. *Science*, **334**, 83–86.

Hancock AM, Witonsky DB, Gordon AS *et al.* (2008) Adaptations to Climate in

795        Candidate Genes for Common Metabolic Disorders. *PLoS Genet*, **4**, e32.

Hedrick PW, Ginevan ME, Ewing EP (1976) Genetic Polymorphism in Heterogeneous Environments. *Annual Review of Ecology and Systematics*, **7**, 1–32.

Hereford J (2009) A Quantitative Survey of Local Adaptation and Fitness Trade-Offs. *The American Naturalist*, **173**, 579–588.

800      Hijmans RJ, Cameron SE, Parra JL, Jones PG, Jarvis A (2005) Very high resolution interpolated climate surfaces for global land areas. *International Journal of Climatology*, **25**, 1965–1978.

Hoban S, Kelley JL, Lotterhos KE *et al.* (2016) Finding the Genomic Basis of Local Adaptation: Pitfalls, Practical Solutions, and Future Directions. *The American*

805      *Naturalist*, **188**, 379–397.

Hoffmann MH (2002) Biogeography of Arabidopsis thaliana (L.) Heynh. (Brassicaceae). *Journal of Biogeography*, **29**, 125–134.

Horton MW, Hancock AM, Huang YS *et al.* (2012) Genome-wide patterns of genetic variation in worldwide Arabidopsis thaliana accessions from the RegMap

810      panel. *Nat Genet*, **44**, 212–216.

Horton MW, Willems G, Sasaki E, Koornneef M, Nordborg M (2016) The genetic architecture of freezing tolerance varies across the range of Arabidopsis thaliana. *Plant, Cell & Environment*, **39**, 2570–2579.

Hunter DJ (2005) Gene-environment interactions in human diseases. *Nat Rev Genet*,

815      **6**, 287–298.

Jarquín D, Crossa J, Lacaze X *et al.* (2014) A reaction norm model for genomic selection using high-dimensional genomic and environmental data. *Theoretical and Applied Genetics*, **127**, 595–607.

Jones FC, Grabherr MG, Chan YF *et al.* (2012) The genomic basis of adaptive

820      evolution in threespine sticklebacks. *Nature*, **484**, 55–61.

36

Kang HM, Sul JH, Service SK *et al.* (2010) Variance component model to account for sample structure in genome-wide association studies. *Nat Genet*, **42**, 348–354.

Kang HM, Zaitlen NA, Wade CM *et al.* (2008) Efficient Control of Population Structure in Model Organism Association Mapping. *Genetics*, **178**, 1709–1723.

Kawecki TJ, Ebert D (2004) Conceptual issues in local adaptation. *Ecology Letters*, **7**, 1225–1241.

Keller MC (2014) Gene × Environment Interaction Studies Have Not Properly Controlled for Potential Confounders: The Problem and the (Simple) Solution. *Temperament: Genetic and Environmental Factors*, **75**, 18–24.

Keller SR, Levsen N, Olson MS, Tiffin P (2012) Local Adaptation in the Flowering-Time Gene Network of Balsam Poplar, Populus balsamifera L. *Molecular Biology and Evolution*, **29**, 3143–3152.

Kim K-C, Lai Z, Fan B, Chen Z (2008) Arabidopsis WRKY38 and WRKY62 Transcription Factors Interact with Histone Deacetylase 19 in Basal Defense. *The Plant Cell Online*, **20**, 2357–2371.

Kim S, Plagnol V, Hu TT *et al.* (2007) Recombination and linkage disequilibrium in Arabidopsis thaliana. *Nat Genet*, **39**, 1151–1155.

Kooperberg C, Dai JY, Hsu L (2016) Two-stage procedures for the identification of gene x environment and gene x gene interactions in genome-wide association studies. In: *Statistical approaches to gene x environment interactions for complex phenotypes*, pp. 11–34. MIT Press, Cambridge, Massachusetts.

Korte A, Vilhjalmsson BJ, Segura V *et al.* (2012) A mixed-model approach for

845        genome-wide association studies of correlated traits in structured

populations. *Nat Genet*, **44**, 1066–1071.

Landguth EL, Cushman SA (2010) cdpop: A spatially explicit cost distance

population genetics program. *Molecular Ecology Resources*, **10**, 156–161.

Langlet O (1971) Two hundred years genecology. *Taxon*, 653–721.

850     Lasky JR, Des Marais DL, McKay JK *et al.* (2012a) Data from: Characterizing genomic

variation of Arabidopsis thaliana: the roles of geography and climate.

Lasky JR, Des Marais DL, Lowry DB *et al.* (2014) Natural variation in abiotic stress

responsive gene expression and local adaptation to climate in Arabidopsis

thaliana. *Molecular Biology and Evolution*, **31**, 2283–2296.

855     Lasky JR, Des Marais DL, McKay JK *et al.* (2012b) Characterizing genomic variation

of Arabidopsis thaliana: the roles of geography and climate. *Molecular

Ecology*, **21**, 5512–5529.

Lasky JR, Upadhyaya HD, Ramu P *et al.* (2015) Genome-environment associations in

sorghum landraces predict adaptive traits. *Science Advances*, **1**, e1400218.

860     Leimu R, Fischer M (2008) A Meta-Analysis of Local Adaptation in Plants. *PLoS ONE*,

**3**, e4010.

Levene H (1953) Genetic Equilibrium When More Than One Ecological Niche is

Available. *The American Naturalist*, **87**, 331–333.

Levy Karin E, Wicke S, Pupko T, Mayrose I (2017) An Integrated Model of

865     Phenotypic Trait Changes and Site-Specific Sequence Evolution. *Systematic

biology*.

Li Y, Cheng R, Spokas KA, Palmer AA, Borevitz JO (2014) Genetic Variation for Life History Sensitivity to Seasonal Warming in Arabidopsis thaliana. *Genetics*, **196**, 569–577.

870    Lotterhos KE, Whitlock MC (2014) Evaluation of demographic history and neutral parameterization on the performance of FST outlier tests. *Molecular Ecology*, **23**, 2178–2192.

Lovell JT, Juenger TE, Michaels SD *et al.* (2013) Pleiotropy of FRIGIDA enhances the potential for multivariate adaptation. *Proceedings of the Royal Society B:*
875    *Biological Sciences*, **280**, 20131043.

Lowry D, Behrman K, Grabowski P *et al.* (2014) Adaptations between ecotypes and along environmental gradients in Panicum virgatum. *The American Naturalist.*

Lowry DB, Willis JH (2010) A Widespread Chromosomal Inversion Polymorphism
880    Contributes to a Major Life-History Transition, Local Adaptation, and Reproductive Isolation. *PLoS Biol*, **8**, e1000500.

Manel S, Holderegger R (2013) Ten years of landscape genetics. *Trends in Ecology & Evolution*, **28**, 614–621.

Marigorta UM, Gibson G (2014) A simulation study of gene-by-environment
885    interactions in GWAS implies ample hidden effects. *Frontiers in Genetics*, **5**.

Mitchell-Olds T, Willis JH, Goldstein DB (2007) Which evolutionary processes influence natural genetic variation for phenotypic traits? *Nat Rev Genet*, **8**, 845–856.

39

Murayama M, Hayashi S, Nishimura N *et al.* (2012) Isolation of Arabidopsis ahg11, a

890        weak ABA hypersensitive mutant defective in nad4 RNA editing. *Journal of Experimental Botany*, **63**, 5301–5310.

Murcray CE, Lewinger JP, Gauderman WJ (2009) Gene-Environment Interaction in Genome-Wide Association Studies. *American Journal of Epidemiology*, **169**, 219–226.

895    Nordborg M, Weigel D (2008) Next-generation genetics in plants. *Nature*, **456**, 720–723.

van Oppen MJH, Oliver JK, Putnam HM, Gates RD (2015) Building coral reef resilience through assisted evolution. *Proceedings of the National Academy of Sciences*, **112**, 2307–2313.

900    Price AL, Zaitlen NA, Reich D, Patterson N (2010) New approaches to population stratification in genome-wide association studies. *Nat Rev Genet*, **11**, 459–463.

Pyhäjärvi T, Hufford MB, Mezmouk S, Ross-Ibarra J (2013) Complex Patterns of Local Adaptation in Teosinte. *Genome Biology and Evolution*, **5**, 1594–1609.

905    Rao CR (1971) Minimum variance quadratic unbiased estimation of variance components. *Journal of Multivariate Analysis*, **1**, 445–456.

Reimherr M, Nicolae D (2015) Estimating Variance Components in Functional Linear Models with Applications to Genetic Heritability. *Journal of the American Statistical Association*, 00–00.

910    Rellstab C, Gugerli F, Eckert AJ, Hancock AM, Holderegger R (2015) A practical guide to environmental association analysis in landscape genomics. *Molecular Ecology*, **24**, 4348–4370.

Schaffer HE, Johnson FM (1974) ISOZYME ALLELIC FREQUENCIES RELATED TO SELECTION AND GENE-FLOW HYPOTHESES. *Genetics*, **77**, 163–168.

915    Schoville SD, Bonin A, François O *et al.* (2012) Adaptive Genetic Variation on the Landscape: Methods and Cases. *Annual Review of Ecology, Evolution, and Systematics*, **43**, 23–43.

Schrider DR, Mendes FK, Hahn MW, Kern AD (2015) Soft Shoulders Ahead: Spurious Signatures of Soft and Partial Selective Sweeps Result from Linked Hard

920    Sweeps. *Genetics*, **200**, 267–284.

Sharbel TF, Haubold B, Mitchell-Olds T (2000) Genetic isolation by distance in Arabidopsis thaliana: biogeography and postglacial colonization of Europe. *Molecular Ecology*, **9**, 2109–2118.

Shindo C, Aranzana MJ, Lister C *et al.* (2005) Role of FRIGIDA and FLOWERING

925    LOCUS C in Determining Variation in Flowering Time of Arabidopsis. *Plant Physiol.*, **138**, 1163–1173.

Shoji T (2014) ATP-binding cassette and multidrug and toxic compound extrusion transporters in plants: A common theme among diverse detoxification mechanisms. *Int Rev Cell Mol Biol*, **309**, 303–346.

930    Slatkin M (1973) GENE FLOW AND SELECTION IN A CLINE. *Genetics*, **75**, 733–756.

Stinchcombe JR, Weinig C, Ungerer M *et al.* (2004) A latitudinal cline in flowering time in Arabidopsis thaliana modulated by the flowering time gene FRIGIDA.

*Proceedings of the National Academy of Sciences of the United States of America*, **101**, 4712–4717.

935     Szechyńska-Hebda M, Czarnocka W, Hebda M, Karpiński S (2016) PAD4, LSD1 and EDS1 regulate drought tolerance, plant biomass production, and cell wall properties. *Plant Cell Reports*, 1–13.

Thomas D (2010) Methods for Investigating Gene-Environment Interactions in Candidate Pathway and Genome-Wide Association Studies. *Annual review of*

940     *public health*, **31**, 21–36.

Tiezzi F, de los Campos G, Parker Gaddis KL, Maltecca C (2017) Genotype by environment (climate) interaction improves genomic prediction for production traits in US Holstein cattle. *Journal of Dairy Science*, **100**, 2042–2056.

945     Tiffin P, Ross-Ibarra J (2014) Advances and limits of using population genetics to understand local adaptation. *Trends in Ecology & Evolution*, **29**, 673–680.

Toomajian C, Hu TT, Aranzana MJ *et al.* (2006) A Nonparametric Test Reveals Selection for Rapid Flowering in the Arabidopsis Genome. *PLoS Biol*, **4**, e137.

Turner TL, Bourne EC, Von Wettberg EJ, Hu TT, Nuzhdin SV (2010) Population

950     resequencing reveals local adaptation of Arabidopsis lyrata to serpentine soils. *Nat Genet*, **42**, 260–263.

Verslues PE, Lasky JR, Juenger TE, Liu T-W, Kumar MN (2014) Genome-Wide Association Mapping Combined with Reverse Genetics Identifies New Effectors of Low Water Potential-Induced Proline Accumulation in

955     Arabidopsis. *Plant Physiology*, **164**, 144–159.

Voight BF, Kudaravalli S, Wen X, Pritchard JK (2006) A Map of Recent Positive Selection in the Human Genome (L Hurst, Ed,). *PLoS Biology*, **4**, e72.

Weigel D, Nordborg M (2015) Population Genomics for Understanding Adaptation in Wild Plant Species. *Annual Review of Genetics*, **49**, 315–338.

960    Wilczek AM, Cooper MD, Korves TM, Schmitt J (2014) Lagging adaptation to warming climate in Arabidopsis thaliana. *Proceedings of the National Academy of Sciences*, **111**, 7906–7913.

Windle M (2016) *Statistical Approaches to Gene X Environment Interactions for Complex Phenotypes*. MIT Press.

965    Wituszyńska W, Ślesak I, Vanderauwera S *et al.* (2013) LESION SIMULATING DISEASE1, ENHANCED DISEASE SUSCEPTIBILITY1, and PHYTOALEXIN DEFICIENT4 Conditionally Regulate Cellular Signaling Homeostasis, Photosynthesis, Water Use Efficiency, and Seed Yield in Arabidopsis. *Plant Physiology*, **161**, 1795–1805.

970    Yates F, Cochran WG (1938) The analysis of groups of experiments. *The Journal of Agricultural Science*, **28**, 556–580.

Yeaman S, Whitlock MC (2011) THE GENETIC ARCHITECTURE OF ADAPTATION UNDER MIGRATION–SELECTION BALANCE. *Evolution*, **65**, 1897–1911.

Yoder JB, Stanton-Geddes J, Zhou P *et al.* (2014) Genomic Signature of Adaptation to

975    Climate in Medicago truncatula. *Genetics*.

Zomer RJ, Trabucco A, Bossio DA, Verchot LV (2008) Climate change mitigation: A spatial analysis of global land suitability for clean development mechanism

afforestation and reforestation. *Agriculture, Ecosystems & Environment,* **126,**

67–80.

980 **Data Accessibility**

All data were previously published, including fitness (Data Dryad package (Fournier-

Level *et al.* 2011b), environment (Data Dryad package (Lasky *et al.* 2012a), and SNPs

(Horton *et al.* 2012), available at http://bergelson.uchicago.edu/wp-

content/uploads/2015/04/call_method_75.tar.gz). Simulation data previously published in

985 (Forester *et al.* 2016) are archived in Data Dryad package (Forester BR *et al.* 2015). New

simulation data, and code for simulations and GWAS are included in an online

supplemental file with this manuscript.


**Author contributions**

990 JRL designed research and led paper writing. All authors conducted analyses and

contributed to writing.

44

**Table 1**. Characterization of patterns in *Arabidopsis* case study identified by Approach 4 (mixed model including imputations) for SNPs in 0.01 lower tail of p-values for SNP×environment interactions for fitness (first two rows of table) and for kinship×environment interactions for fitness (third row). SNPs with home allele advantage are defined as those where the sign of allelic differences in home climates were mirrored by the sign of fitted mixed model SNP×environment associations with relative fitness. Rank changing SNPs are those where we estimated a rank change in relative fitness for alternate alleles along the environmental gradient between the two extreme common gardens. The final row gives the proportion of total observed climate gradient (among ecotypes) captured by the two most extreme common gardens.

| *Statistic* | *Aridity* | *CV grow. seas. prec.* | *Min. temp.* | *Min. temp. grow. seas.* |
|---|---|---|---|---|
| Proportion SNP×E with home allele advantage | 0.46 | 0.89 | 0.92 | >0.99 |
| Proportion SNP×E rank changing | 0.31 | 0.92 | >0.99 | 0.73 |
| Kinship×E $R^2$ for fitness | 0.08 | 0.58 | 0.07 | 0.43 |
| Proportion climate gradient covered by gardens | 0.13 | 0.65 | 0.78 | 0.31 |

45

**Table 2**. Permutation tests of enrichment p-values (Approach 4) for various signals suggestive of local adaptation to climate in case study on *Arabidopsis*. For each statistic, we tested for enrichment of signal in the SNPs in the 0.01 lower tail of p-values for SNP×environment associations with relative fitness. "Genic" tests enrichment of genic versus non-genic SNPs, "PHS" and "iHS" test for enrichment with significant (alpha = 0.05) pairwise haplotype sharing and standardized integrated extended haplotype homozygosity, respectively. The final row shows enrichment with SNPs having significant (alpha = 0.05) associations with change in flowering time (G×E) in response to warming during growth.

| *Statistic* | *Aridity enrichment* | *CV grow. seas. prec. enrichment* | *Min. temp. enrichment* | *Min. temp. grow. seas. enrichment* |
|---|---|---|---|---|
| Genic | 0.0036 | <0.0002 | 0.0054 | 0.0006 |
| PHS | 0.0272 | 0.0122 | 0.0068 | 0.0272 |
| iHS | 0.2840 | 0.0006 | 0.0020 | 0.0008 |
| Flowering time under warming, G×E | 0.8582 | 0.0680 | 0.5844 | <0.0002 |

1010

1015

46

**Figure 1.** Illustration of our imputation technique and stereotypical patterns captured by our approach for neutral (top panels) and selected (bottom panels) loci. Here we show hypothetical data from four common gardens along an environmental gradient (solid circles in four vertical streaks in right panels, with small amount of noise added to environmental values for visualization) that have fitness scaled to a maximum of 1. We also show accessions (or ecotypes) collected in home environments and sequenced (mapped in two-dimensional geographical space in left panels) having imputed relative fitness of 1 in their home environment (environment-of-origin, open circles at top of right panels). The selected locus (bottom right panel) in question shows strong G×E for fitness, such that allele *B* (blue) is more fit (observed, solid circles) and more common (imputed, open circles) at the upper end (right side) of the environmental gradient while allele *b* (orange) is more fit and more common at the lower end (left side) of the gradient.



47
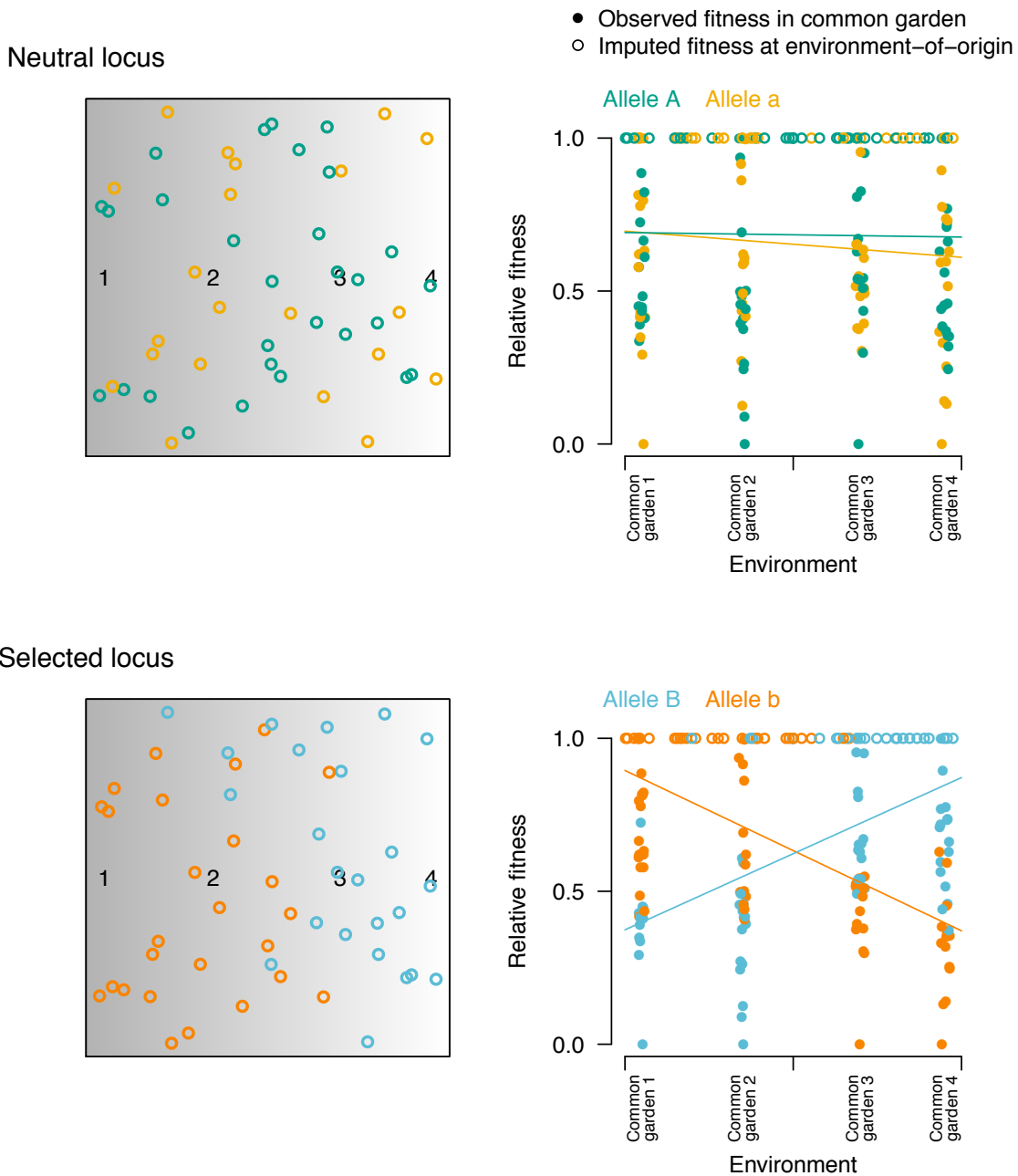
1030   **Figure 2**. Data used in case study on *Arabidopsis*. The location of common gardens, natural accessions in common gardens, and all other sequenced natural accessions are shown.
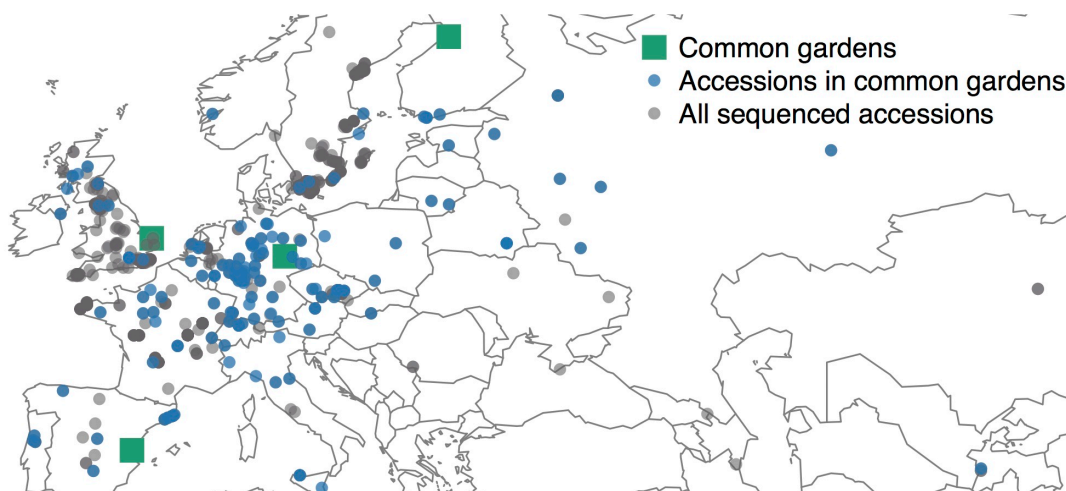
1035     **Figure 3.** Comparison of inferred causal (red) and neutral (black) SNP associations with G×E for fitness across three different levels of dispersal and 10 replicate simulations for each level. Approaches used (row 1) no imputation and no random effects, (row 2) imputation but no random effects, (row 3) mixed models that used only observations from four common gardens, (row 4) mixed models combining imputed observations of relative fitness in home environments with

1040     common garden observations, or (row 5) a genotype-environment association approach. False positive rate (FPR) is indicated, calculated as the proportion of simulations where a neutral SNP had the lowest p-value. Each simulation had 1 causal SNP and 99 neutral SNPs; plots show aggregate distributions for all SNP by simulation combinations (*i.e.* total of 10 causal and 990 neutral SNPs). Y-axes show the proportion of SNPs in each category (causal or neutral) falling

1045     into a given p-value bin. For reference, dashed line indicates a strict Bonferroni cutoff for alpha = 0.05, $-\log(0.05/100) = 7.6$.
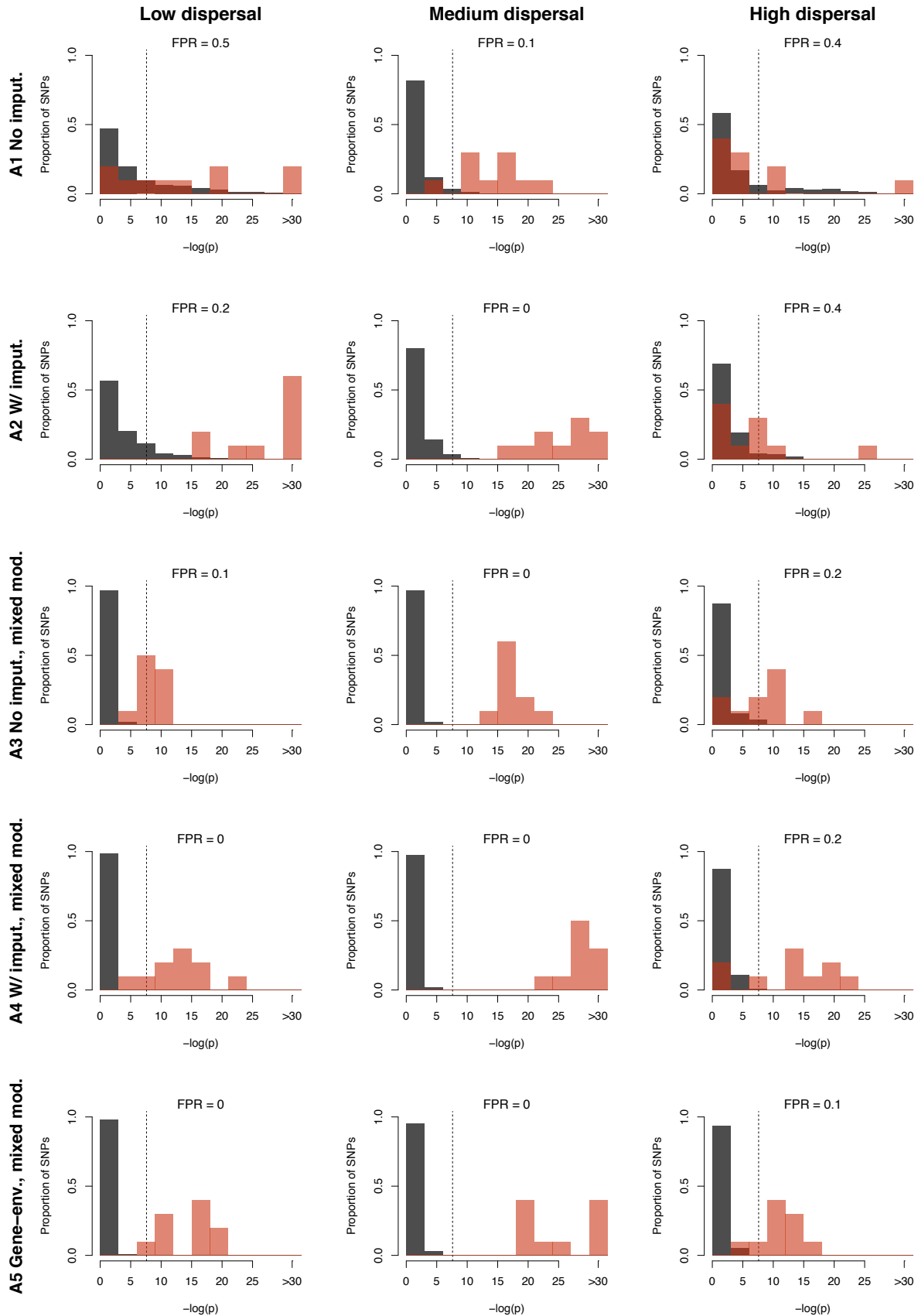
1050     **Figure 4**. Example SNPs with the strongest associations (lowest p-values) with cold winter temperatures (A) and aridity (B). Top subpanels show the climate distribution of alleles in home genotypes (natural geographic patterns), known as genotype-environment associations. Bottom subpanels show relative fitness of alleles in four common gardens, where common gardens' climates determine position on x-axes. Each SNP falls within the coding region of indicated

1055     genes (WRKY38 and LSD1). Box widths are scaled to relative number of accessions having each allele. In both (A) and (B), the allele with the greatest relative fitness in common gardens changes along the environmental gradient consistent with change in allele frequency in native accessions (i.e. ecotypes).

## A. WRKY38 (Chr. 5, pos. 7496047)
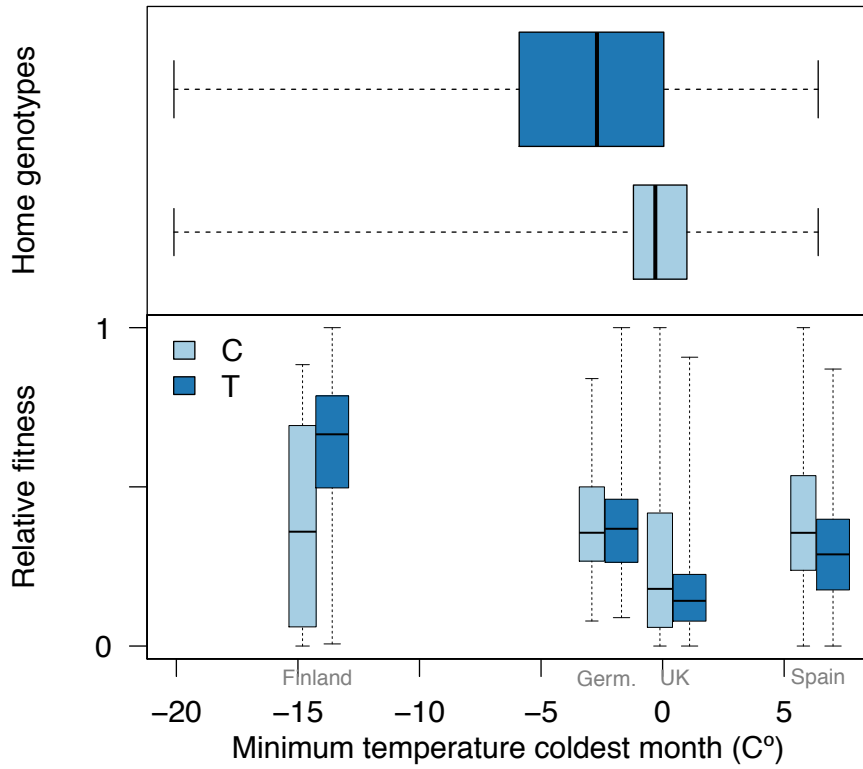


## B. LSD1 (Chr. 4, pos. 11005059)
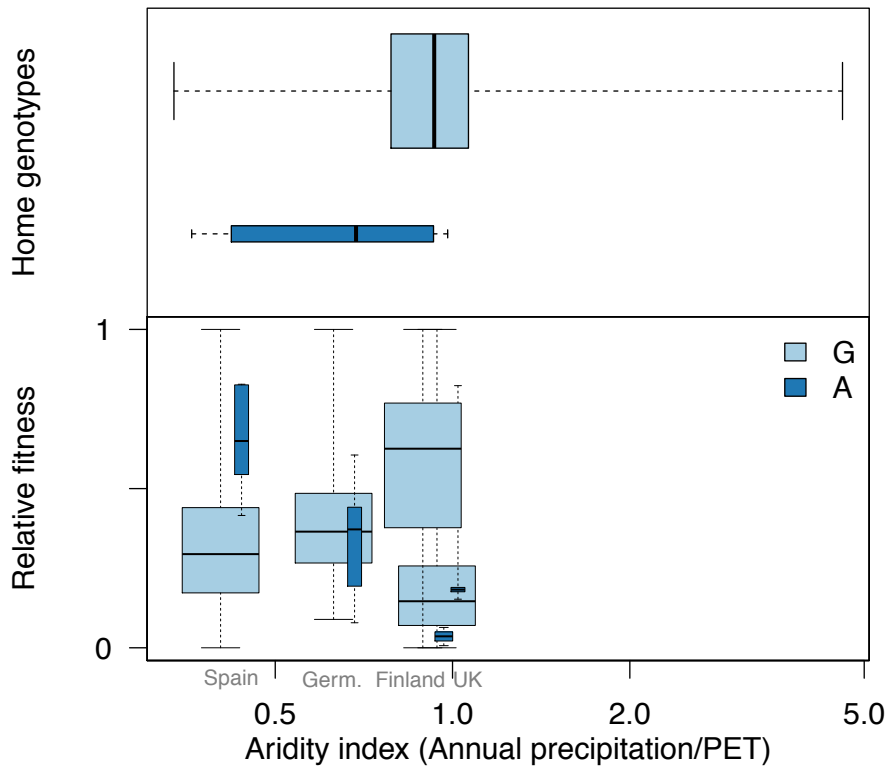
1060 **Supporting information**

**Tables S1-S4 (attached csv files)**. List of genes within 1 kb of SNPs in the lower 0.001

quantile for p-values for SNP×environment interactions for each climate variable,

including imputed observations and accounting for kinship.

1065

**Table S5**. Rank correlation among SNPs for SNP×environment effect p-values comparing three tested approaches (Approaches 2-4) with Arabidopsis.

| | Random effect, no imputation | Random effect, imputation |
|---|---|---|
| **Min. temp. growing season** | | |
| *No random effect, including imputation* | 0.396 | -0.001 |
| *Random effect, no imputation* | | 0.041 |
| | | |
| **Aridity** | | |
| *No random effect, including imputation* | 0.318 | 0.008 |
| *Random effect, no imputation* | | -0.032 |
| | | |
| **Min. temp. coldest month** | | |
| *No random effect, including imputation* | -0.021 | -0.012 |
| *Random effect, no imputation* | | 0.104 |
| | | |
| **CV growing season prec.** | | |
| *No random effect, including imputation* | 0.178 | 0.090 |
| *Random effect, no imputation* | | -0.006 |

1070 **Table S6.** Overlap (one-tailed permutation tests) and rank correlations (Spearman's rho) between our approach (Approach 4, mixed-model with imputation, climate variables give row labels at left) and published approaches to identifying SNPs associated with local adaptation in Arabidopsis. Citations are given for the original publication of previous approaches. For partial Mantel and RDA, we used absolute value of SNP scores to rank

1075 SNPs. Empty cells indicate climate variables not tested in Hancock et al. (2011).

| Climate var. | Mixed model, overlap in 0.01 tail strongest associations | Mixed model, rank correlation between associations | Partial Mantel, overlap in 0.01 tail strongest associations | Partial Mantel, rank correlation between associations | First axis of RDA, overlap in 0.01 tail strongest associations | First axis of RDA, rank correlation between associations | First axis of RDA after removing spatial structure, overlap in 0.01 tail strongest associations | First axis of RDA after removing spatial structure, rank correlation between associations |
|---|---|---|---|---|---|---|---|---|
| | Lasky et al. 2014 | Lasky et al. 2014 | Hancock et al. 2011 | Hancock et al. 2011 | Lasky et al. 2012 | Lasky et al. 2012 | Lasky et al. 2012 | Lasky et al. 2012 |
| Min. temp. growing season | <0.0001 | 0.079 | | | 0.0489 | -0.093 | <0.0001 | -0.132 |
| Aridity | <0.0001 | 0.028 | <0.0001 | 0.065 | <0.0001 | -0.015 | 0.1107 | 0.013 |
| Min. temp. coldest month | <0.0001 | 0.042 | 0.0128 | 0.044 | <0.0001 | -0.213 | <0.0001 | -0.057 |
| CV growing season prec. | <0.0001 | 0.187 | | | 0.9591 | -0.028 | 0.9953 | 0.030 |

**Figure S1**. Example outcome of selection on a simulated landscape under moderate dispersal (maximum dispersal of 10% of the landscape surface per generation), with

1080     selective gradient (grayscale background), 250 randomly sampled accessions (small circles), and four common gardens (green squares). 100 accessions were simulated in the four common gardens (i.e. reciprocal transplant) covering the full gradient (large light green squares) and in four gardens covering only half the gradient (smaller dark green squares).
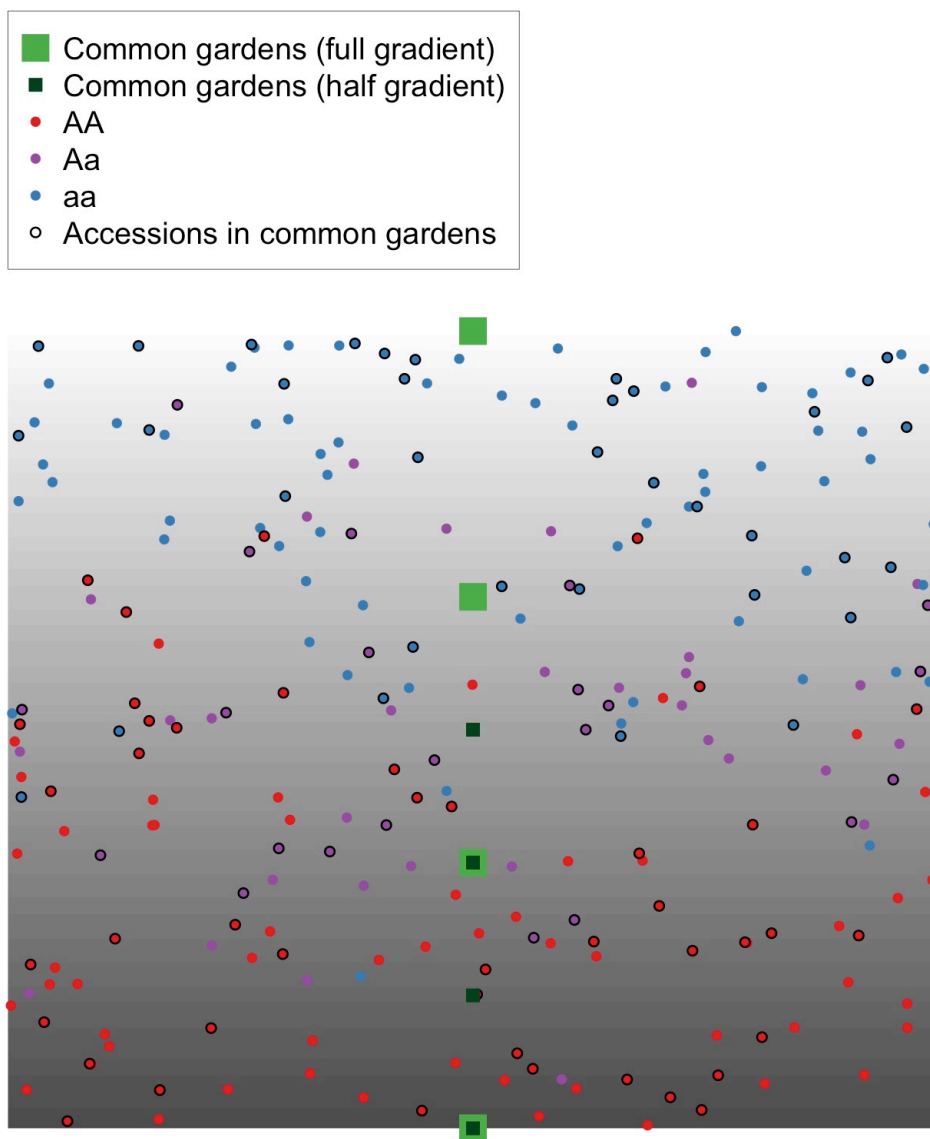
1085

**Figure S2.** Example outcome of selection on a simulated landscape under low dispersal (maximum dispersal of 3% of the landscape surface per generation), with selective gradient (grayscale background), 250 randomly sampled accessions (small circles), and four common gardens (green squares). 100 accessions were simulated in the four common gardens (i.e. reciprocal transplant) covering the full gradient (large light green squares).
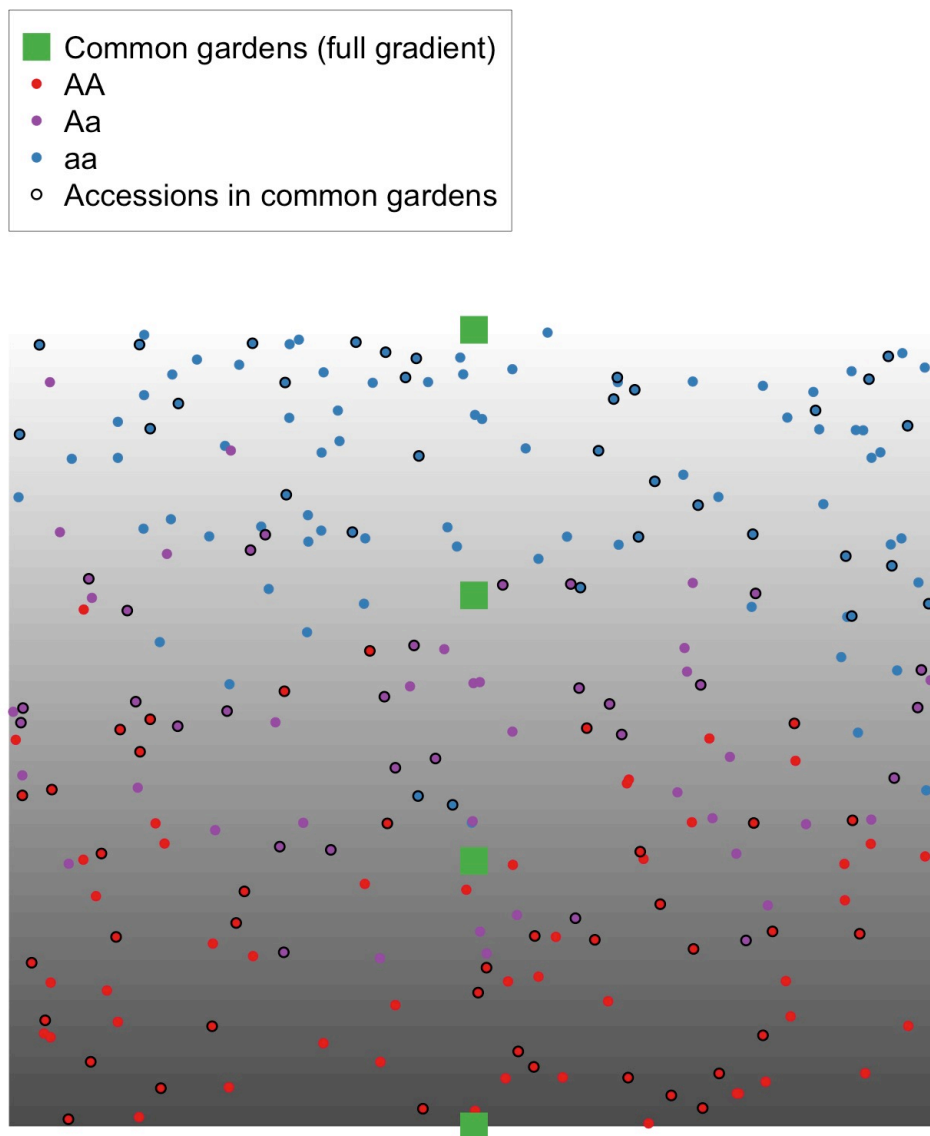
1095     **Figure S3.** Example outcome of selection on a simulated landscape under high dispersal (maximum of 25% of the landscape surface per generation), with selective gradient (grayscale background), 250 randomly sampled accessions (small circles), and four common gardens (green squares). 100 accessions were simulated in the four common gardens (i.e. reciprocal transplant) covering the full gradient (large light green squares).
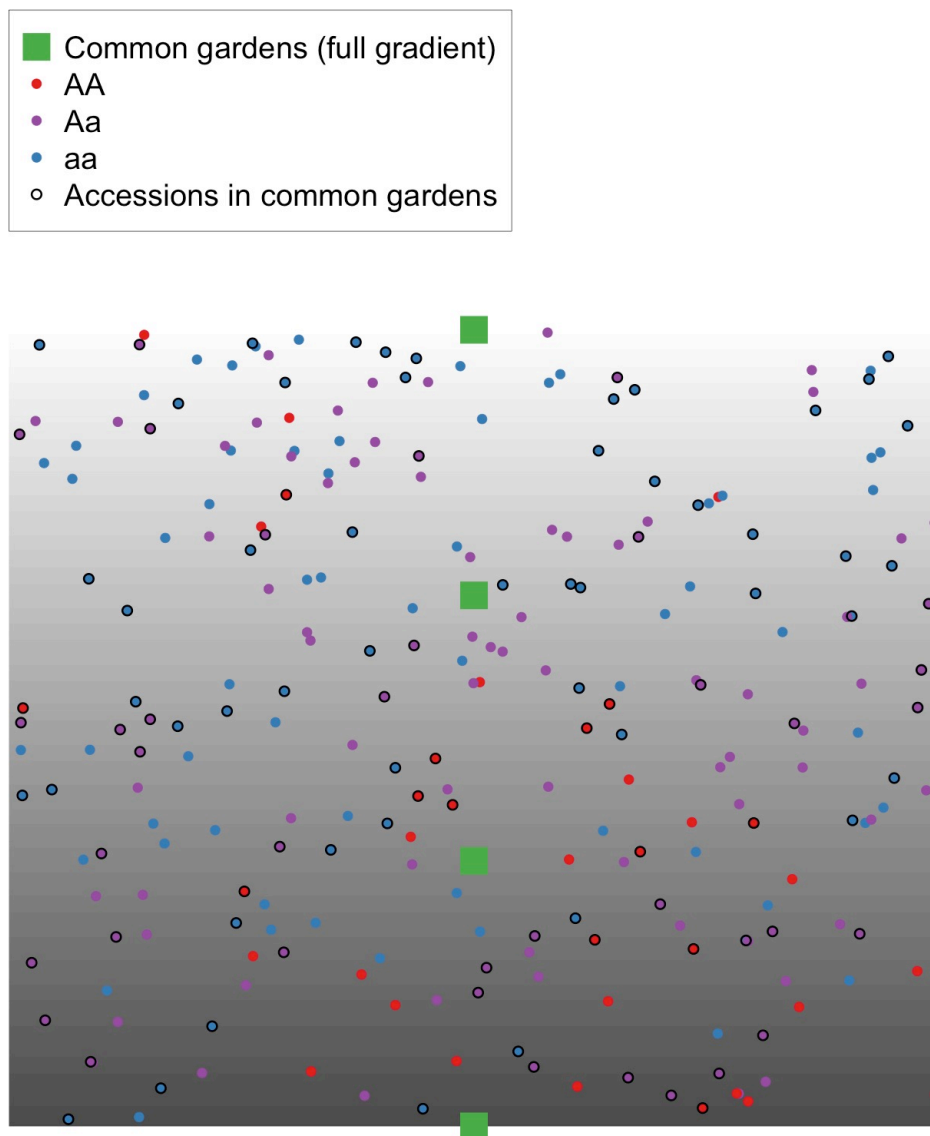


1100

**Figure S4.** Comparison of inferred causal (red) and neutral (black) SNP associations with G×E for fitness across 10 replicate simulations for moderate dispersal with common gardens covering only half the gradient. Approaches used (row 1) no imputation and no random effects, (row 2) imputation but no random effects, (row 3) mixed models that used only observations from four common gardens, or (row 4) mixed models combining imputed observations of relative fitness in home environments with common garden observations. False positive rate (FPR) is indicated, calculated as the proportion of simulations where a neutral SNP had the lowest p-value. Each simulation had 1 causal SNP and 99 neutral SNPs; plots show aggregate distributions for all SNP by simulation combinations (*i.e.* total of 10 causal and 990 neutral SNPs). Y-axes show the proportion of SNPs in each category (causal or neutral) falling into a given p-value bin. For reference, dashed line indicates a strict Bonferroni cutoff for alpha = 0.05, –log(0.05/100) = 7.6.
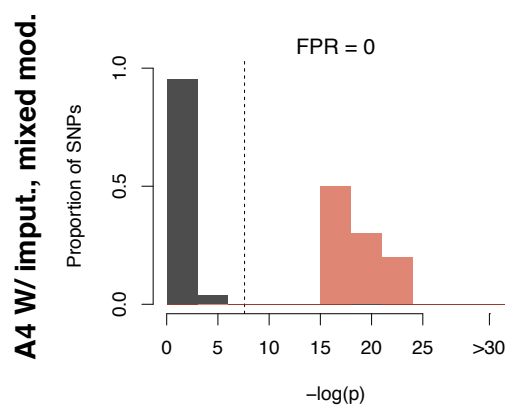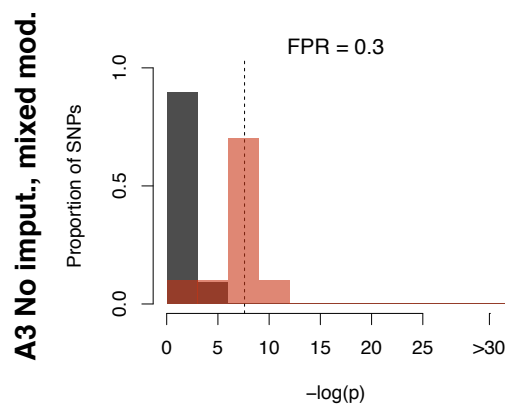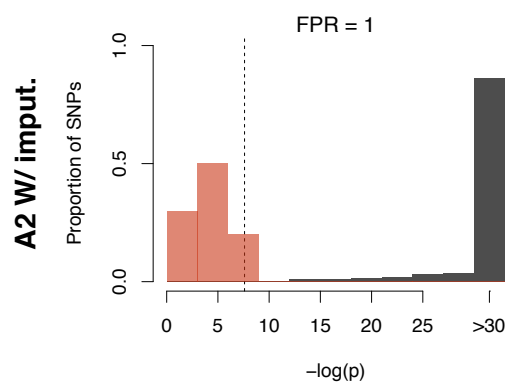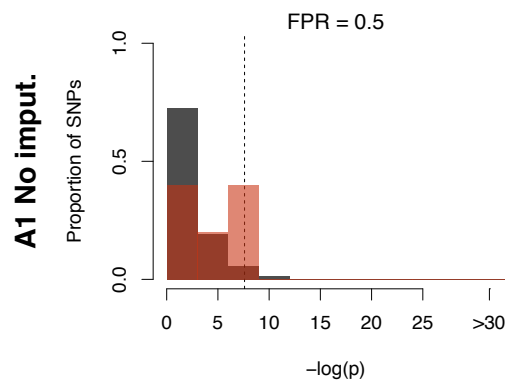
1115 **Figure S5**. Quantile-quantile plots of p-value distributions for four approaches to calculating genome-wide SNP×environment associations with fitness, using published data on *Arabidopsis thaliana*. X-axes show expected $-\log_{10}(p)$ and y-axes show observed $-\log_{10}(p)$. Approaches used (column 1) no imputation and no random effects, (column 2) imputation but no random effects, (column 3) mixed models that used only observations
1120 from four common gardens, or (column 4) mixed models combining imputed observations of relative fitness in home environments with common garden observations.
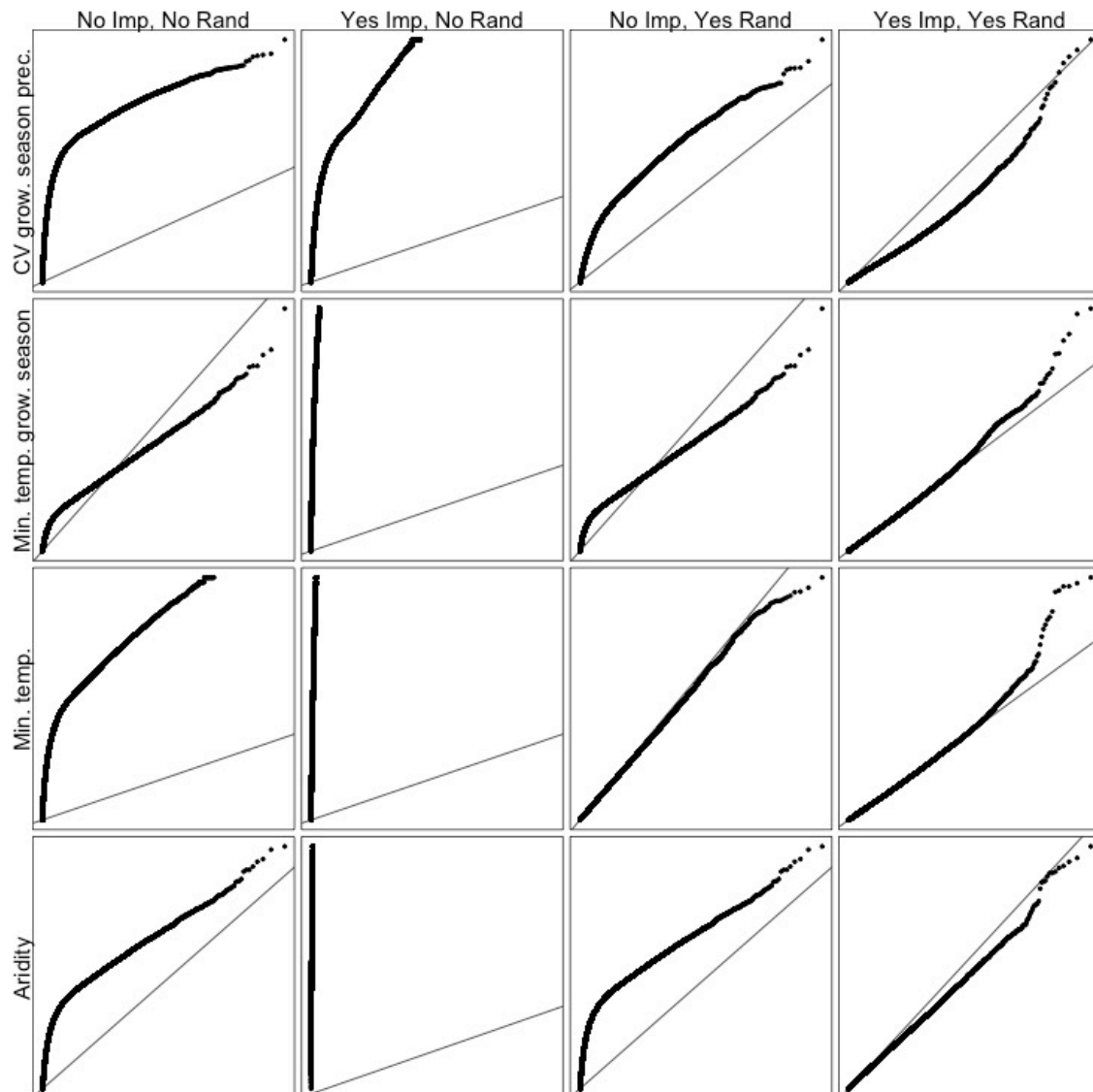
**Figure S6.** Example of fitted effects on fitness of allelic variation at two SNPs (arbitrary

1125    labeled 1 and 2) across two common gardens (arbitrary labeled x and y). In this scenario,

both SNPs exhibit antagonistic pleiotropy (rank changing) across the environmental

gradient. However, each SNP has relatively weaker effects on fitness in one environment.

A test of whether an individual SNP shows the strongest associations with fitness in an

individual garden (*e.g.* SNP 1 at site x) might incorrectly infer conditional neutrality

1130    because other markers show stronger associations (SNP 2 at site x).